

The role of USP19 in denervation induced skeletal muscle wasting

By

Tamara Moore

Department of Medicine

Division of Experimental Medicine

McGill University, Montreal, Quebec, Canada

April 2010

A thesis submitted to McGill University in partial fulfillment of the requirements
of the degree of Masters of Science

© Tamara Moore 2010



Library and Archives
Canada

Published Heritage
Branch

395 Wellington Street
Ottawa ON K1A 0N4
Canada

Bibliothèque et
Archives Canada

Direction du
Patrimoine de l'édition

395, rue Wellington
Ottawa ON K1A 0N4
Canada

Your file *Votre référence*
ISBN: 978-0-494-72798-0
Our file *Notre référence*
ISBN: 978-0-494-72798-0

NOTICE:

The author has granted a non-exclusive license allowing Library and Archives Canada to reproduce, publish, archive, preserve, conserve, communicate to the public by telecommunication or on the Internet, loan, distribute and sell theses worldwide, for commercial or non-commercial purposes, in microform, paper, electronic and/or any other formats.

The author retains copyright ownership and moral rights in this thesis. Neither the thesis nor substantial extracts from it may be printed or otherwise reproduced without the author's permission.

AVIS:

L'auteur a accordé une licence non exclusive permettant à la Bibliothèque et Archives Canada de reproduire, publier, archiver, sauvegarder, conserver, transmettre au public par télécommunication ou par l'Internet, prêter, distribuer et vendre des thèses partout dans le monde, à des fins commerciales ou autres, sur support microforme, papier, électronique et/ou autres formats.

L'auteur conserve la propriété du droit d'auteur et des droits moraux qui protègent cette thèse. Ni la thèse ni des extraits substantiels de celle-ci ne doivent être imprimés ou autrement reproduits sans son autorisation.

In compliance with the Canadian Privacy Act some supporting forms may have been removed from this thesis.

While these forms may be included in the document page count, their removal does not represent any loss of content from the thesis.

Conformément à la loi canadienne sur la protection de la vie privée, quelques formulaires secondaires ont été enlevés de cette thèse.

Bien que ces formulaires aient inclus dans la pagination, il n'y aura aucun contenu manquant.


Canada

TABLE OF CONTENTS	1
LIST OF FIGURES AND TABLES	3
ACKNOWLEDGEMENTS	4
ABSTRACT	6
RÉSUMÉ	8
LIST OF ABBREVIATIONS	10
I. INTRODUCTION	
<i>1.1 Skeletal Muscle Wasting in Disease</i>	11
<i>1.2 The Ubiquitin-Proteasome System</i>	14
<i>1.3 The Role of the Ubiquitin Proteasome System in Muscle Wasting...</i>	19
<i>1.4 Deubiquitinating Enzymes</i>	20
<i>1.5 Functions of Deubiquitinating Enzymes</i>	22
<i>1.6 The Role of USP19 in Skeletal Muscle Wasting</i>	24
II. MATERIALS AND METHODS	
<i>2.1 Generation of USP19 knockout (KO)Mice</i>	26
<i>2.2 Denervation of Hindlimb Muscles</i>	26
<i>2.3 Protein Analysis and DNA quantification</i>	27
<i>2.4 Morphometry</i>	28
III. RESULTS	
<i>3.1 USP19 KO mice have higher muscle mass compared to wild type (WT) littermates</i>	29
<i>3.2 Male USP19 knockout mice lose less muscle mass after denervation than wild type littermates.....</i>	31
<i>3.3 USP19 KO mice sparing is not gender specific</i>	31
<i>3.4 USP19 KO mice lose less muscle protein content than Wild type littermates</i>	34
<i>3.5 USP19 KO mice have higher myofibrillar protein levels after denervation</i>	34

3.6	<i>USP19 KO muscle have more muscle fibers than WT mice</i>	37
3.7	<i>USP19 KO muscle undergoes less apoptosis during denervation ...</i>	41
IV.	DISCUSSION	45
V.	REFERENCES	48

LIST OF FIGURES AND TABLES

FIGURE 1: The contractile components of skeletal muscle.....	12
FIGURE 2: The ubiquitin proteasome system.....	16
TABLE 1: Structure and function of polyubiquitin linkages	18
FIGURE 3: UCH and UBP/USP enzyme conserved regions.....	21
TABLE 2: Male USP19 KO mice lose less mass than Wild type mice in tibialis anterior (TA) and gastrocnemius (GAS) muscles following sectioning of the sciatic nerve.....	30
TABLE 3: Female USP19 KO mice lose less mass than wild type mice in tibialis anterior and GAS muscles following sectioning of the sciatic nerve.....	32
TABLE 4: Mass of mouse organs in male and female USP19 KO and Wild type mice	33
FIGURE 4: Protein content is higher in GAS muscle in male USP19 KO mice than Wild type mice	35
FIGURE 5: Tropomyosin and MHC protein is higher in GAS muscles of USP19 KO mice compared to WT mice 14 days after severing the sciatic nerve	36
FIGURE 6: Light microscopy images of immunohistochemical stain of type I, IIA and IIB MHC in WT and KO GAS of mice severed at the sciatic nerve	38
FIGURE 7: Distribution of cross sectional areas of GAS fiber from Wildtype and USP19 KO mice post denervation	39
FIGURE 8: The cross sectional area of GAS fiber types from Wildtype and USP19 KO mice post denervation	42
FIGURE 9: Male USP19 KO mice lose less DNA content and show less PARP cleavage than WT mice when undergoing severing of the sciatic nerve	43

ACKNOWLEDGEMENTS

I would like to thank the individuals who have assisted me during this portion of my academic life, whose advice, guidance and resources made it possible for me to complete my Masters. First and foremost, I would like to thank God for having brought me this far in life. May everything I do be His will.

I would like to thank Dr. Simon Wing, my supervisor, for his gentle encouragement of my intellectual development over the past two years. Under his coaching, my skills as a critical thinker have been honed. His knowledge and gift for teaching has refined my ability to analyse results and answer scientific queries in a logical and rational manner. Moreover, I am grateful for his compassionate nature and his propensity to develop his students as well rounded individuals. Though he continues to wear many hats, as supervisor, director and clinician, his busy schedule has not damaged the quality of my training and has increased my respect for him. I continue to appreciate his concern for my well being academically and personally.

I would like to thank Nathalie Bedard, head technician, for her invaluable lab training and her assistance in all my knockout mouse studies. I am grateful for her patience when teaching me and her meticulous organization of the lab, both of which facilitated my experiments immensely. I also owe a debt of gratitude to Yu Lu, PhD student, for providing me with tips for optimizing experiments as well as insight into my results. I truly enjoyed our debates on topics ranging from the results of journal club papers to the philosophical questions of life. I also would like to thank Marie Plourde, for her abundant supply of knockout mice for my many experiments, without which my project would have been impossible. To my fellow colleagues Miao Miao, Priyanka Sundaram and Yaoming Yang, I thank you for the many happy conversations we have shared. You have all truly enriched my experience in this lab.

I would also like to thank the labs that collaborated with me on various aspects of my project. I am grateful to Pat Halluer and Dr. Kenneth Hastings for giving me their time and resources. Their guidance allowed me to master new

techniques, such as mouse surgery and tissue sectioning.

Finally, I would like to thank those who encouraged me to persevere even in the wake of setbacks: my loving and supportive fiancé Curtis Brissette, my mother Isabelle Moore, my closest friend Pamela Steinman and Madison Baptist Church Bible Study. I am truly grateful for their prayers and support.

ABSTRACT

Skeletal muscle wasting can be a fatal complication of many diseases, such as cancer, AIDS and neuromuscular disorders. During wasting, the ubiquitin-proteasome system (UPS) is the primary pathway for the catabolism of myofibrillar proteins. Many studies have explored the importance of enzymes mediating the conjugation of ubiquitin to muscle proteins. However, the role of deubiquitinating enzymes in skeletal muscle wasting is poorly understood. Our laboratory previously identified USP19 as a deubiquitinating enzyme which is upregulated in response to atrophic stimuli *in vivo* and is capable of indirectly regulating the expression of myofibrillar proteins in muscle cells *in vitro*. However, the role of USP19 during skeletal muscle wasting *in vivo* remains unexplored. To address this question, I have characterized the phenotype of USP19 KO mice and determined the effects of denervation induced wasting of hindlimb muscles of USP19 KO mice by measuring various anatomical and structural parameters. Denervation stimulus was chosen to minimize number of animals used since control and treated limbs are within the same animal. USP19 KO mice had slightly heavier gastrocnemius muscle (GAS) mass than WT mice, with a trend towards a larger fiber size and higher protein content. After denervation, the skeletal muscle mass of KO mice is 30% heavier than that of denervated WT mice in both the tibialis anterior (TA) and GAS muscle. This significant sparing is correlated with KO having 30% more protein than WT in GAS muscles, after denervation. The level of the myofibrillar protein tropomyosin was significantly higher in denervated KO GAS than in denervated WT GAS, consistent with previous USP19 siRNA studies in rat skeletal muscle cells. Although, structural analysis of denervated GAS fiber reveals a small but significant sparing in the fiber size of KO mice as compared to WT mice, this difference only accounts for 5% of the mass sparing observed in KOs. Loss of neural stimulation in muscle is known to induce apoptosis during atrophy. My biochemical analysis showed that denervation results in less DNA loss in KO

GAS muscles when compared to WT GAS muscles. In addition, there was a decrease in the levels of apoptotic markers, caspase-3 and Poly-ADP-Ribose-Polymerase (PARP) cleavage, in denervated KO GAS as compared to denervated WT GAS. Taken together, this evidence suggests that the muscle sparing occurs via a novel mechanism, where USP19 deletion promotes skeletal fiber survival after loss of neuronal stimulation. Therefore, USP19 could be a therapeutic target in the treatment of muscle wasting disorders.

RÉSUMÉ

L'atrophie musculaire est une grave complication qui peut être fatale dans plusieurs maladies comme le cancer, le SIDA ou les maladies neuromusculaires. Le système ubiquitine-protéasome (UPS) est le mécanisme le plus impliqué dans la dégradation des protéines myofibrillaires durant l'atrophie. Plusieurs études ont démontré l'importance de certaines enzymes catalysant la conjugaison de l'ubiquitine aux protéines musculaires. Parcontre, le rôle des enzymes de déubiquitination durant l'atrophie musculaire est encore très peu connu. Notre laboratoire a précédemment identifié USP19, une enzyme de déubiquitination, qui est régulée à la hausse en réponse à plusieurs stimuli d'atrophie musculaire *in vivo* et qui est aussi capable de réguler indirectement des protéines myofibrillaires dans des cellules musculaires *in vitro*. Toutefois, le rôle de USP19 dans l'atrophie musculaire *in vivo* est encore inconnu. Afin d'aborder cette question, j'ai caractérisé le phénotype de souris dont le gène USP19 a été inactivé (KO) et j'ai déterminé les effets d'une dénervation des muscles de la patte postérieure sur ces souris KO en mesurant divers paramètres anatomiques et structuraux. Les souris USP19 KO possèdent une masse du muscle gastrocnemius (GAS) légèrement plus grande que les souris contrôles (WT) avec une tendance vers des fibres plus grosses et un contenu protéique plus élevé. Après dénervation, les muscles squelettiques des souris KO étaient 30% plus lourds que ceux des souris WT et ce dans le GAS ainsi que dans le tibialis postérieur (TA). Cette économie significative corrèle bien avec une augmentation de 30% du contenu protéique dans les muscles KO (GAS) comparé aux muscles WT, après dénervation. Aussi, les niveaux de la protéine myofibrillaire tropomyosine étaient significativement plus élevés dans le GAS KO que dans le GAS WT, après dénervation, ce qui est consistant avec des études postérieures de siRNA contre USP19 dans des cellules musculaires de rat. Bien que des analyses structurales des GAS dénervés aient démontré une faible mais significative économie dans la taille des fibres KO comparé aux fibres WT, cette différence ne peut justifier que pour 5% de

l'économie de masse musculaire observée dans les souris KO. Par ailleurs, la perte de stimulation neurale dans les muscles est reconnue pour induire l'apoptose durant l'atrophie. Mes analyses biochimiques ont démontré une perte d'ADN moins importante dans les muscles GAS KO que dans les WT après dénervation. De plus, nous avons observé une diminution des taux des marqueurs d'apoptose caspase-3 et de poly-ADP-ribose-polymerase (PARP), dans les muscles GAS dénervés KO comparé aux GAS dénervé WT. Dans l'ensemble, ces résultats suggèrent que l'économie de masse musculaire observée se produit via un nouveau mécanisme où la perte de USP19 favorise la survie des fibres squelettiques après une coupure de la stimulation neuronale. Par conséquence, USP19 pourrait être utilisé comme cible thérapeutique dans le traitement des maladies liées à l'atrophie musculaire.

List of Abbreviations:

AMSH-LP = AMSH-like protease

Con = Control

CSA = Cross sectional Area

Den = Denervation

DUB = deubiquitinating enzymes

E1 = Ubiquitin activating enzyme

E2 = Ubiquitin conjugating enzyme

E3 = Ubiquitin protein ligase

ECL = Enhanced Chemiluminescence

EDL = Extensor Digitorum Longus

ERAD = Endoplasmic Reticulum Associated Protein Degradation

GAS = Gastrocnemius

JAMM = Jab1/MPN domain-associated metalloisopeptidase

KO = Knockout

MJD = Josephin/Machado-Joseph disease

MHC = Myosin Heavy Chain

MRF = Myogenic Regulatory Factor

MURF = Muscle-specific Ring Finger

OTU = Ovarian tumour domain proteins

PARP = Poly-ADP-Ribose-Polymerase

PVDF = Polyvinylidene fluoride

RING = Really Interesting New Gene

TA = Tibialis Anterior

Ub = Ubiquitin

UCH = ubiquitin carboxy-terminal hydrolases

UPS = Ubiquitin Proteasome System

USPs/UBPs = Ubiquitin specific proteases

WT = Wildtype

I. INTRODUCTION

1.1 Skeletal Muscle Wasting in Disease

Skeletal muscle is a tissue comprised primarily of protein, the nature of which mediates a variety of essential functions, such as ambulation, respiration and energy storage. Skeletal muscle wasting is an important complication of many diseases. Anorexia, kidney failure, neuromuscular disease, diabetes mellitus, sepsis, AIDS, cancer, Cushing's syndrome and hyperthyroidism are all conditions accompanied by a net decrease in skeletal muscle protein (review in ¹). These conditions can cause muscle mass and protein content to fall below the threshold required to maintain respiratory muscles, resulting in death. Severe muscle loss is known as muscle wasting and is a component of cachexia². Muscle wasting can occur locally such as in decreased innervation of specific muscles or can be systemic such as during prolonged glucocorticoid treatment³. Regardless of the initiating factors, the skeletal muscle wasting is the result of a net negative balance in the rates of protein synthesis and protein degradation⁴.

During muscle wasting, mass may be lost as a result of muscle cell atrophy or cell death. Muscle atrophy is the reduction in myofiber volume accompanied by a loss in protein content and disorganization of muscle structure characterized by striations within the cell⁵. Alternatively, muscle mass may decrease as a result of necrosis or apoptosis. Studies report the increase of apoptotic markers such as Bax, cleaved PARP, and DNA fragmentation, in the GAS, following sectioning of the sciatic nerve in the rat⁶. Stimulating myogenesis could potentially counteract the loss of muscle wasting resulting from increased cell death.

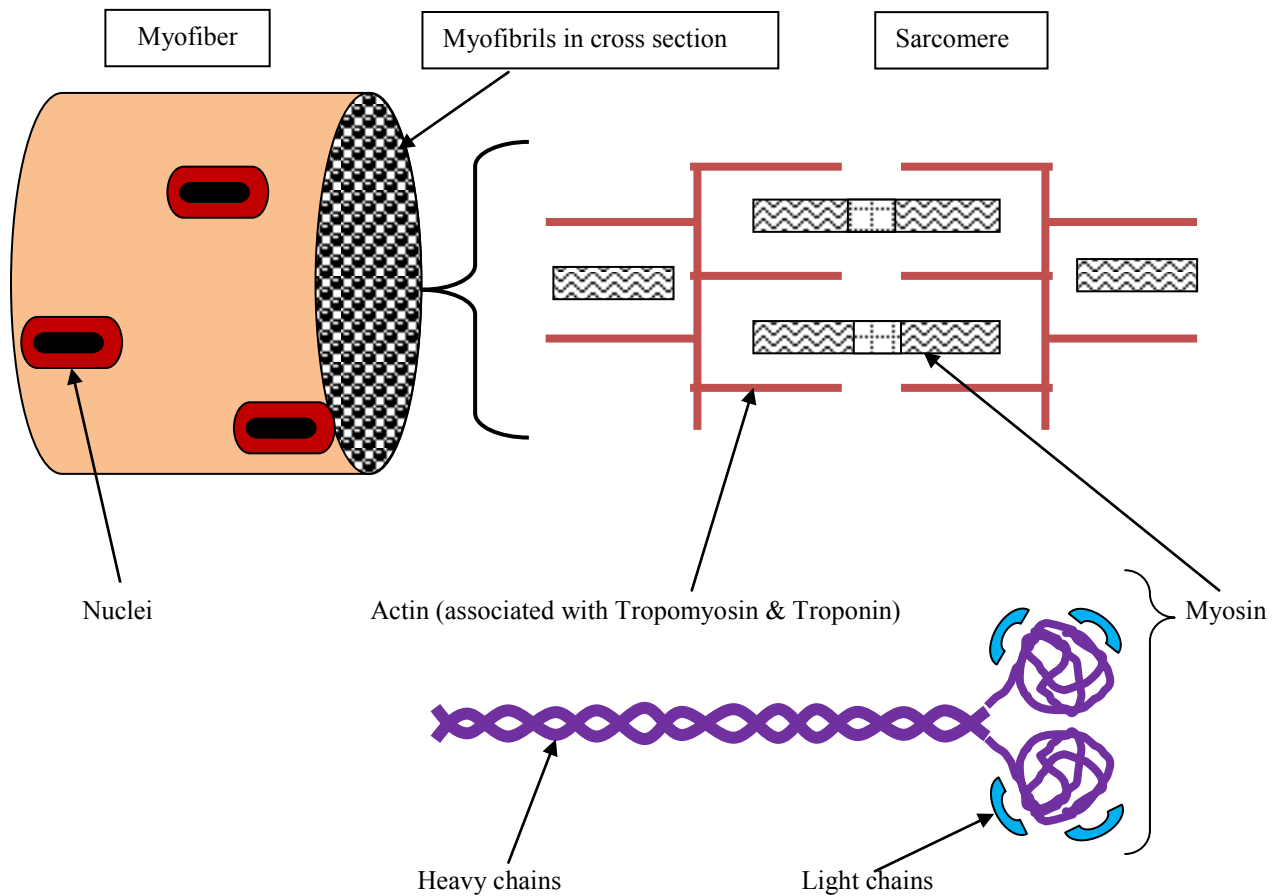


Figure 1: The contractile components of skeletal muscle. Skeletal muscle is made up of a series of multinucleated myofibers, each with several peripheral nuclei. Each myofiber contains many myofibrils which are comprised of sarcomeres in series. The sarcomere is the contractile unit of muscle. In the sarcomere, actin thin filaments and myosin thick filaments overlap with each other, forming the striations of skeletal muscle. The myosin thick filament is composed of 2 heavy chains and 4 light chains. Myosins are arranged together in a side by side complex.

Myogenesis refers to the process by which muscle differentiates. Although most muscle is formed during embryonic development, adult skeletal muscle maintains plasticity. This flexibility allows for changes in protein content in response to stimuli, such as feeding, fasting, exercise and injury. In the case of muscle injury, stem cells can replenish the damaged tissue via a process known as muscle regeneration. In mature mammalian muscle, mononuclear stem cells/satellite cells will move from the basal lamina to the site of injury and undergo differentiation to muscle precursor cells. These precursor cells are known as myoblasts. The myoblasts will fuse into multinucleated cells, known as myotubes, which terminally differentiate into myofibers⁷. Cells committed to myogenesis express the myogenic regulatory factors (MRFs): MyoD, Myf-5, myogenin, and MRF4⁸. These MRFs are transcription factors, expressed in a temporal manner. The MRFs belong to the superfamily of basic helix-loop-helix transcription factors, which have been shown to heterodimerize with E proteins and bind DNA E-box motifs found in the promoters of many skeletal muscle-specific genes⁹.

Muscle is predominantly composed of the myofibrillar proteins, myosin and actin, with less abundant levels of accessory proteins such as tropomyosin and troponin¹⁰. These proteins are organized into filaments, forming the contractile apparatus of muscle, known as the sarcomere (Figure 1). The sarcomere has thick and thin filaments. Thick filaments consist of myosin and thin filaments are comprised of actin, tropomyosin and troponin. Muscle contraction begins when troponin binds to calcium and initiates the interaction of actin and myosin. The muscle contracts because thick and thin filaments move over each other in an ATP-dependant manner¹¹. It has been demonstrated that myofibrillar proteins decrease during wasting, as seen in the rodent models of sciatic nerve denervation or treatment with cortisone³. Since muscle function requires sufficient myofibrillar proteins to maintain the highly-organized infrastructure of the sarcomere, understanding the mechanism of protein depletion is critical to reversing muscle wasting in humans.

Mammalian skeletal muscle contains four myosin isoforms. Most fibers contain one myosin isoform, designating the fiber type. Muscles can be characterized by determining the abundance of these four fiber types: I, IIA, IID/X and IIB. There is a correlation between ATPase activity and myosin isoforms such that type I fibers are slower than type II fibers, having less ATPase activity than type II fibers¹². In addition, fibers may switch isoforms by moving from I ↔ IIA ↔ IID/X ↔ IIB. Hybrid fibers exist in low abundance and are the result of fiber type transitions. Hybrid fibers may contain only two adjacent isoforms of myosin in the switching program described above. In C57Jbl/6 mice, fast-twitch muscles such as the extensor digitorum longus (EDL), tibialis anterior (TA) and GAS muscles, contain mostly type IIB fibers (55-65% of total fibers). These type IIB fibers in EDL, TA and GAS have the largest cross-sectional area. Conversely, slow-twitch muscles like the soleus (SOL) are predominantly type I and IIA fibers (~40% each of total fibers) with the largest cross sectional area attributed to type I fibers (all ref¹³).

It has been shown that changes in fiber cross-sectional area can accurately represent the extent of muscle atrophy or hypertrophy¹⁴. A study on denervated EDL in rats reports a dramatic decrease in the cross-sectional area of type IIA and IIB fibers (42% and 36% loss of area, respectively), while the I and IIX fibers are less affected by denervation, decreasing their average cross-sectional area by only 9% and 13%, respectively¹⁵. Taken together, gross skeletal muscle anatomy in fast twitch muscle is most influenced by changes in the largest and most abundant fibers such as the type IIB fibers.

1.2 The Ubiquitin-Proteasome System

Although, proteins may be degraded by calcium dependant proteases and lysosomal proteases, inhibition of these pathways are not sufficient to reverse the protein loss which occurs during skeletal muscle atrophy¹⁶. However inhibition of the proteasome can inhibit the increase in proteolysis in atrophying skeletal muscle, as was demonstrated in a rodent model of diabetes¹⁷. Therefore, the ubiquitin-proteasome system (UPS) is regarded as the major pathway for protein

degradation in skeletal muscle cells.

Ubiquitin (Ub) is an 8kDa protein containing 76 amino acids. The UPS degrades proteins which are conjugated to polymers of Ub. Ub chains have been shown to target their attached substrate to the 26S proteasome for degradation. In order to generate Ub chains, Ub monomers are covalently attached to a lysine (K) residue on a substrate or on a previously conjugated Ub¹. The process requires the sequential action of three enzymes: Ub-activating enzyme (E1), Ub-conjugating enzyme (E2) and Ub-ligase (E3). Initially, the carboxyl end of Ub is activated by E1 through the hydrolysis of ATP. This step results in the Ub forming a thiol-ester linkage with a cysteine residue in the active site of the E1 (Figure 2). The activated ubiquitin is then transferred to a specific E2. Lastly, the glycine 76 carboxyl group in the C-terminus of Ub is coupled to the ϵ -amino group of lysine of the substrate or preceding ubiquitin. This last step is catalyzed by the E2/E3 complex¹⁸.

Substrate specificity is primarily dependent on the E3. To date, two classes of E3 have been identified, Really Interesting New Gene (RING) ligases and homology to E6AP C-Terminus (HECT) ligases. If the E3 contains a RING finger domain, as is the case for muscle-specific RING finger-1 (MURF-1), the substrate will be selected by the E3, which recruits and activates the E2 for transfer of the Ub to the substrate¹⁹. If the E3 contains a HECT domain, such as KIAA10 found in human muscle, the Ub will be transferred from the E2 to the E3 and subsequently conjugated to the substrate by the E3^{20, 21}.

E3s can exist as multimeric protein complexes. The SCF ligase complex is composed of a Cullin, Skp, and F-box protein. In the complex, Cull1 N-terminus interacts with Skp1 while Cull1 C-terminus interacts with Rbx1/Roc1/Hrt1; thus Cull1 serves as a scaffolding protein. Rbx1/Roc1/Hrt1 contains the RING domain for binding the E2. The RING domain mediates the transfer of Ub from the E2 to the substrate²². The F-box protein is bound to Skp1 and serves as a receptor to recruit specific protein substrates to SCF complexes. The F-box is located at the N-terminal of F-box proteins. In addition, the protein may contain, at the C-terminus, a variety of other motifs such as WD40 repeats, leucine-rich repeats,

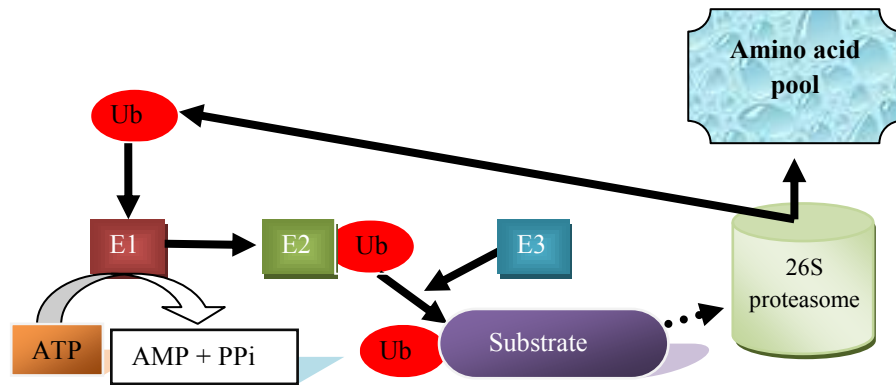


Figure 2: The Ubiquitin Proteasome System. The E1 hydrolyses ATP into AMP and pyrophosphate which activates the ubiquitin moiety. Ubiquitin (Ub) enters the pathway by binding to the cysteine in the active site of the Ub-activating-enzyme (E1). The ubiquitin is transferred to the Ub-conjugating-enzyme (E2) which recruits the Ub ligase (E3). The E3 selects substrates and forms linkages. The linkage is formed with one of seven lysine residues in Ub, which is dictated by the E2/E3 pair involved. Finally, the E3 catalyzes the formation of the isopeptide bond between the ϵ -amino group of lysine (K) on the substrate or Ub and the glycine residue at position 76 of the ubiquitin. If Ubs are linked via K48, the substrate is targeted to the proteasome. Proteolysis in the proteasome requires hydrolysis of ATP to ADP and Pi.

kelch repeats, carbohydrate-interacting motifs, and proline-rich regions. An example of a SCF ligase in muscle is, MAFbx, which is responsible for MyoD degradation²³.

Ub can accept the covalent attachment of an additional Ub on any lysine residues within its amino acid sequence. Since Ub contains 7 lysine residues there are 7 potential linkage variations, resulting in branched chains of polyubiquitin (Table 1). These branched chains may contain one or more linkage types. Certain E2/E3s catalyze the formation of specific linkages. Early studies of Ub chains has led to the generalization that K48 linked chains target the substrate for degradation by the proteasome, while other linkages regulate protein function or sub-cellular localization. However, recent studies in yeast, suggest that other lysine linkages have been underestimated in their abundance and may also play a role in substrate degradation²⁴.

Polyubiquitinated proteins with a minimum of four Ub are reported to be recognized and degraded by the 26S proteasome. The 26S proteasome is composed of the 20S proteasome and 19S regulatory complex. The 20S proteasome is a cylindrical stack of subunits arranged in four rings. These rings are comprised of seven alpha and seven beta subunits, with the former on the exterior and the latter on the interior. The alpha subunits are non-catalytic, the beta subunits are catalytic. The 20S proteasome contains three distinct catalytic activities which are similar to the proteases chymotrypsin, trypsin and caspase. However, in contrast to these latter proteases, the proteasome is a threonine based protease. The 19S regulatory complexes bind the alpha-rings of the 20S proteasome. The 19S complex is comprised of six ATPases which generate the energy for 26S proteasome assembly and twelve non-ATPase subunits. Finally, the degraded peptides are extruded from the proteasome (rev in²⁵).

Although this project focuses on protein degradation it should be noted that ubiquitination (in particular monoubiquitination) of proteins can regulate many cellular processes, such as, membrane trafficking, transcriptional regulation and DNA repair and replication²⁶.

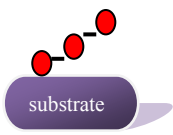
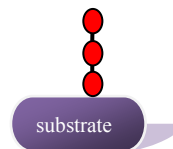
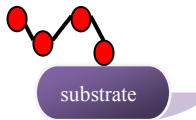
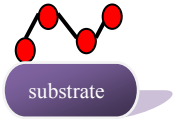
Linkage	Stereochemistry	Cellular Abundance in Yeast	Attributed function
Monoubiquitin		Unknown	membrane trafficking transcriptional regulation DNA repair
Multiple monoubiquitins			DNA replication Histone modulation
K48		29%	Targeting to 26S proteasome
K63		16%	Endosomal trafficking Kinase activation DNA damage response Stress response Ribosomal function
K29		3%	Targeting to proteasome
K6		10%	Targeting to proteasome (yeast)
K11	uncharacterized	28%	
K33	uncharacterized	3.5%	
K27	uncharacterized	9%	

Table 1: Structure and function of polyubiquitin linkages Examples of ubiquitin chains formed in vivo²⁶. The ubiquitin (red) is covalently attached to a lysine residue on the substrate or the specified lysines of the preceding ubiquitin. Cellular abundance reported in yeast^{24,27}.

1.3 The Role of the Ubiquitin Proteasome System in Muscle Wasting

The UPS is thought to play a prominent role during muscle atrophy since many of its components increase during wasting despite net protein loss. As a result, normally long-lived myofibrillar proteins, actin and myosin, have an accelerated breakdown. Since these two proteins constitute 60 - 70 percent of total muscle protein, their loss leads to muscular weakness²⁸. In humans, it was reported that the UPS is the major regulator of muscle wasting during its early stages however chronic wasting conditions results in a depression of protein synthesis and the upregulation of other mechanisms of proteolysis²⁹.

Within the UPS induced protein degradation, specific E2s and E3s have been shown to target myofibrillar proteins for degradation. Fielitz *et al.* showed that the E3s muscle RING finger-1(MuRF) and MuRF3 cooperate with the E2, UbcH5, to degrade β -myosin heavy chain (MHC) and MHCIIa in mice. Mice deficient in both MuRF1 and MuRF3 accumulate myosin protein³⁰. There are supporting studies on E3s that show mice lacking either MAFbx or MuRF1 are particularly resistant to atrophic stimuli. Fiber size and muscle mass are larger in the GAS of MAFbx and MuRF1 KO mice 14 days post-denervation when compared to wild-type control mice³¹. These studies indicate a prominent role for ubiquitination during muscle wasting.

In addition, muscle cell culture studies support a role for the UPS in catabolism. Overexpression of the E3, Atrogin-1/MaFbx, causes atrophy in myotubes and has been shown to induce muscle wasting by increasing the proteolysis of myogenic regulatory factor, MyoD^{4, 32}. Consistent with this, components of the UPS are increased in the presence of catabolic stimuli. Proteasomal subunits C2, C5, as well as Ub are upregulated at the mRNA and protein levels when catabolic stimuli are applied to muscle cells in culture³³.

In vivo studies link muscle protein catabolism to an upregulation of the components of the UPS pathway. Some reports in humans, have demonstrated an increase in the levels of mRNA encoding ubiquitin and subunits of proteasome in muscle during sepsis and cancer^{34,35}. Yimlamai *et al.* showed hindlimb unweighting-induced atrophy in rats increases proteolysis and upregulates Ub

conjugates, Ub-conjugating enzyme E2_{14K}, and 20S proteasome activity. The increase was more dramatic in the slow-twitch fibers of the soleus than in fast-twitch muscles, such as the plantaris and tibialis anterior³⁶. E2_{20K} and UBC4/UBC5 are other E2 enzymes which are upregulated during muscle atrophy. Similarly, certain E3 enzymes are more abundant in muscle during wasting. E3alpha found in muscle cells, is induced in cancer cachexia³⁷ and sepsis³⁸ models. E3alpha/UBR1 has been shown to partner with E2_{14K}. Although, there is strong evidence for up-regulation of these enzymes, neither E2_{14K} nor E3alpha is essential for muscle wasting since disruption of either gene fails to reverse the decrease in muscle mass^{39, 40}. Together, these findings imply that enzymes involved in Ub conjugation may not be the sole mechanism for regulating myofibrillar protein degradation during atrophy.

1.4 Deubiquitinating Enzymes

The reverse process of ubiquitin conjugation is deubiquitination. A large body of studies have assessed the roles of enzymes involved in Ub conjugation in mediating myofibrillar protein catabolism. However, protein ubiquitination can also be modulated by deubiquitinating enzymes (DUB), which remain relatively poorly studied. In mammals there are approximately 90 DUBs mediating the hydrolysis of the peptide bond between Ubs and Ub-substrates⁴¹. To date, DUBs may be sub-categorized into one of five groups based on the homology of conserved regions within the enzyme: ubiquitin carboxy-terminal hydrolases (UCH); ubiquitin specific proteases (USPs/UBPs); the ovarian tumour (OTU) domain proteins; the Josephin/Machado-Joseph disease (MJD) proteins and the Jab1/MPN domain-associated metalloisopeptidase (JAMM)²⁶. The first four are cysteine proteases; however the JAMM proteins are zinc metalloproteases.

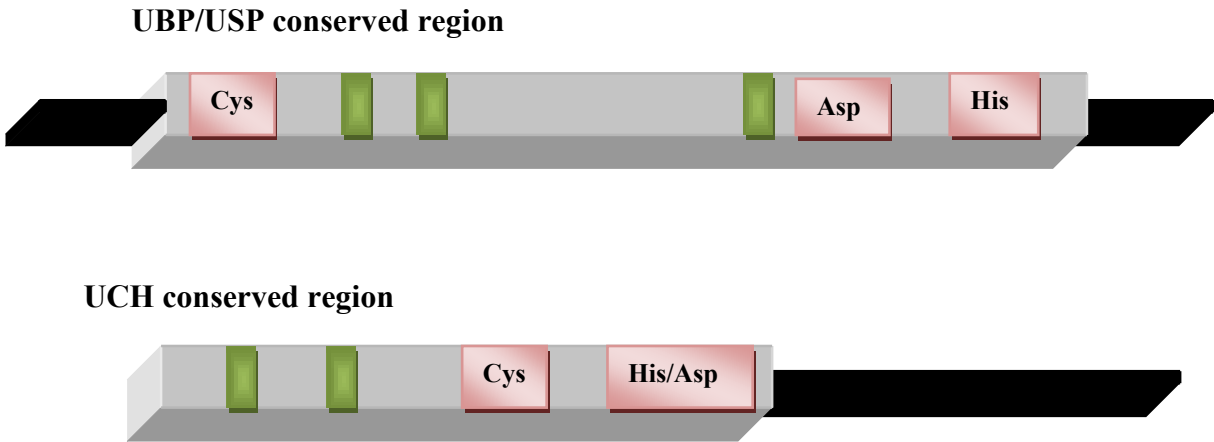


Figure 3: UCH and UBP/USP enzyme conserved regions. The catalytic site cysteine (Cys), Histidine (His) and Aspartate (Asp) are found in both USP and UCH enzymes. In addition USP contains four highly conserved regions (green) located in a 450 amino acid region (grey). Extensions at the amino and carboxy terminus may be present (black).

To date, the human genome encodes 63 USP/UBPs. The USP/UBPs are the largest subfamily of DUB with a conserved core domain that is approximately 300-400 residues in length. These residues encompass 6 conserved motifs including the active site cysteine, histidine and aspartic acid residues (Figure 2). UCH's are similar to the USP/UBPs in overall structure. The UCH cysteine, histidine and aspartic acid residues have been shown to act together in a catalytic mechanism comparable to that found in the cysteine proteases, such as papain/cathepsin B, whereby the charged groups on the histidine and aspartic acid side chain enhances the nucleophilic properties of the thiol on the cysteine residue, allowing the thiol to attack the peptide bond¹⁸.

1.5 Functions of deubiquitinating enzymes

DUBs have many functions. In general terms, they can be viewed as reversing the effects of conjugation and thereby negatively regulating degradation by the proteasome or other non-proteolytic functions of ubiquitination or as depolymerising chains of ubiquitin to maintain the supply of free Ub.

Poly-Ub cleavage requires a DUB. Newly synthesized Ub is translated as a fusion protein of either multiple Ubs or Ub bound to a ribosomal protein. Certain DUBs will process Ub precursors into monomers for use in conjugation reactions. After protein degradation, Ub chains are processed into monomers by Ub pools are thus replenished in vivo. Proteasome-associated DUB, USP5, is an example of DUB with the aforementioned function. USP5 has been shown to cleave only unanchored polyUb chains. Suppression of USP5 results in an increased level of unanchored polyubiquitin chains. In this way, USP5 mediates the recycling of Ub and prevents the accumulation of K48-linked polyUb chains⁴². Interestingly, Otubain1 is a DUB which can cleave free or bound K48-linked polyubiquitin but not other polyubiquitin chains⁴³. Therefore Otubain1 has a dual function, to affect substrate stability and to replenish the pool of Ub monomers.

DUBs may also act on specific Ub linkages to modify non-proteolytic functions. One such example is found in the human JAMM containing DUB,

AMSH-LP, which is reported to preferentially cleave K63 linked chains during endosomal trafficking but which does not cleave K48 chains⁴⁴. The action of AMSH-LP demonstrates that it is a chain selective DUB. AMSH-LP expression is required for the fusion of multivesicular bodies with lysosomes. Other DUBs have been implicated in the regulation of newly synthesized proteins. It is estimated that 30–80% of the newly synthesized proteins are misfolded and therefore must be degraded⁴⁵. This process of quality control is referred to as the endoplasmic reticulum-associated degradation (ERAD) pathway. Overexpression of Ataxin 3 leads to an accumulation of ERAD substrates, such as CD3delta, in a process mediated by ataxin-3's association with VCP/p97⁴⁶. More recently, USP19 was identified as an ER membrane associated protein, able to rescue the ERAD substrate, T-cell receptor alpha from degradation⁴⁷.

Partial chain removal has also been reported as a function of DUBs and this manner may enhance proteasome targeting of the substrate. Multiple Ub can be linked to a single preceding Ub, forming a forked chain. Many E2/E3 enzyme combinations can generate forked Ub chains, *in vitro* and in yeast⁴⁸. Surprisingly, most chains observed *in vivo* are branched not forked. Therefore, these forks may be removed in mammals by DUBs in a process termed “chain editing”. Such “chain editing” DUBs can remove extraneous Ubs linked to off-target lysine residues. For example, Ataxin-3 selectively removes K63 linkages within K48-linked chains. These findings suggest that Ataxin-3 is responsible for ensuring homogenous K48-linked chains, thus enhancing proteasomal degradation of the substrate⁴⁹.

DUBs are heavily associated with the UPS. UCH37 is a DUB associated with the 19S regulatory complex of the proteasome. UCH37 disassembles the distal ends of Ub-chains and thus rescues poorly ubiquitinated or slowly degraded Ub-substrates from proteolysis by the 26S proteasome⁵⁰. A different class of DUB, the JAMM DUB, Rpn11/ POH1 is an essential subunit of the lid subcomplex in the proteasome, and has been shown to remove Ub chains from substrates⁵¹.

The importance of DUBs in regulating protein function and stability has been highlighted in various studies. However the role of DUBs in skeletal muscle

wasting has not been explored. Our lab has identified a DUB which is elevated in skeletal muscle in response to wasting stimuli and which regulates the levels of muscle specific proteins.

1.6 The Role of USP19 in Skeletal Muscle Wasting

USP19 is a 150 kDa protein whose mRNA expression in skeletal muscle has been shown to correlate inversely with the extent of muscle wasting⁵⁰. USP19 is phylogenically conserved. Human USP19 has 81% and 95% amino acid identity with rat and mouse USP19, respectively. During catabolic states, such as glucocorticoid treatment, streptozotocin-induced diabetes, fasting and tumour induction, the levels of USP19 mRNA increase in rat skeletal muscle. This induction of USP19 transcription correlates with a significant decrease in the masses of fast-twitch skeletal muscle, extensor digitorum longus (EDL), tibialis anterior (TA), epitrochlearis and the slow-twitch soleus. Consistent with this, when fasted animals were refed, the transcript levels of USP19 in EDL were decreased. Interestingly, the regulation of USP19 mRNA levels did not fluctuate in the testes, liver or kidney upon fasting, indicating that USP19 regulation is specific to muscle in response to wasting stimuli. This data suggests that USP19 may be important in mediating skeletal muscle atrophy (all in ref⁵²).

Since the levels of USP19 mRNA are inversely correlated to muscle mass, the effects of USP19 depletion were assessed in rat myotubes⁵¹. Silencing USP19 did not alter net cellular protein content. However loss of USP19 protein did decrease the rate of protein degradation by 20% but this reduced rate of degradation was offset by a similar decrease in the rate of protein synthesis. Taken together, this suggests that USP19 inhibits protein synthesis pathways as well as pathways for protein degradation. In the absence of USP19, myofibrillar proteins MHC, actin, and troponin-T, were increased by 1.5 fold while tropomyosin increased most dramatically, by 2.5 fold. Higher protein content could be in part attributed to increased mRNA levels, since both MHC and tropomyosin mRNAs are increased in USP19 depleted cells. Two myogenic regulatory factors, Myf5 and myogenin, are expressed in L6 myotubes. However, only myogenin increased at the protein

and mRNA levels after USP19 depletion. Moreover, MHC protein levels were increased only in the absence of USP19 but not when cells were depleted of both USP19 and myogenin. Taken together, these results show that USP19 negatively regulates the expression and transcription of myofibrillar proteins through a myogenin-dependant mechanism.

In accordance with our previous *in vivo* findings, dexamethasone treated L6 rat myotubes show an increase in USP19. It is known that dexamethasone reduces cellular myosin heavy chain (MHC) in L6 muscle cells. However, this catabolic effect of dexamethasone was prevented in cells lacking USP19. These results show that USP19 is required to lower myofibrillar protein content in myotubes (all in ref ⁵³).

The aforementioned results demonstrate that USP19 is able to indirectly regulate muscle specific genes and proteins *in vitro* and that USP19 transcription increases during states of wasting *in vivo*. In this thesis I explore the role of USP19 in muscle wasting *in vivo*. To answer this question I have characterized the phenotype of USP19 KO mice. Specifically, I have determined the anatomical and biochemical effects of denervation-induced wasting in mice lacking USP19. Denervation stimulus was chosen to minimize number of animals required. In addition control limbs and treated limbs are within the same animal which allows paired statistical analysis. I have examined parameters such as muscle mass and fiber size. Also, I have determined if loss of USP19 affects biochemical indicators of wasting such as overall protein content and specific myofibrillar levels in different fast twitch skeletal muscles. I expect to observe KO mice with higher skeletal muscle mass than WT mice, in part because increased muscle specific proteins were seen in the siRNA studies described above. Moreover, I anticipate less mass and protein loss in USP19 KO mice when exposed to muscle wasting stimuli since L6 muscle cells, depleted of USP19 and exposed to wasting stimuli, had more myofibrillar protein than non-depleted cells under the same conditions.

II MATERIALS AND METHODS:

2.1 Generation of USP19 KO Mice

Embryonic stem cells (BayGenomics) were obtained with a gene trap inserted between exons 2 and 3 of an allele of the USP19 gene. As a result, transcripts are spliced from exon 2 onto the β -galactosidase gene in the b-geo gene trap cassette, rather than onto exon 3 of USP19. This insert occurs before the core domain of USP19 and therefore generates a catalytically inactive, truncated version of USP19 fused to β -galactosidase. The ES cells were injected into blastocysts and implanted in foster mothers. Tail DNA of the progeny was screened by polymerase chain reaction, in order to determine the offspring carrying the disrupted USP19 gene. These recombinant mice were mated with C57bl/6 mice to obtain heterozygotes. Heterozygotes were mated to obtain homozygous mice with the disruption of USP19 after exon 2. These homozygous mice are referred to as USP19KO mice. Disruption of the USP19 gene was confirmed by Western blot and Northern blot using tissue samples from the testis (data not shown). The testis was used to confirm the genotyping results since expression of USP19 protein in muscle is too low to detect reliably. It should be noted that male and female KO mice groups were of disparate ages (9-11 months and 4-8 months respectively) because these mice were the only homozygous offspring available at the time of the studies.

2.2 Denervation of Hindlimb Muscles

Muscle wasting due to decreased neural stimulation was modeled in mice by denervation of the sciatic nerve. Mice were anesthetised by constant inhalation of 2:1 isoflurane and oxygen mixture during operation. A 1 cm incision was made at the lumbar dorsal region on the left and right hind quarters. Denervation was performed by removal of ~0.5 cm section of the sciatic nerve. The contralateral leg served as an internal control. Sham/control operations were performed on the control leg by touching but not severing the sciatic nerve.

Mice were injected, intradermally, with 2 μ l/g body weight Carprofen to

reduce post-operative pain, and approximately 50 µl of lidocaine/bupivacaine was directly applied to the site of incision to provide local anaesthesia. Skin was sutured with metal clamps and Vetbond. Animals were sacrificed by cervical dislocation fourteen days after denervation. The tibialis anterior, GAS, heart, liver and kidneys were immediately weighed and frozen in liquid nitrogen.

2.3 Protein Analysis and DNA quantification

Mouse skeletal muscles were harvested post-mortem, snap frozen in liquid nitrogen and stored at -80°C. Part of the GAS was weighed then homogenized in 1 ml lysis buffer (2% SDS, 50 mM Tris-HCl pH 8) using a Polytron tissue homogenizer. DNA in the sample was sheered by passing it through a 23 gauge syringe. Sheered samples were stored at -20°C. Total muscle protein concentration was determined using BCA Micro Protein Assay (Thermo Fisher Scientific). DNA was quantified by the fluorometric assay PicoGreen (Invitrogen). Fluorescent excitation wavelength was 480 nm and emission wavelength was 520 nm - 590 nm.

To quantify of MHC and tropomyosin levels, 3 µg of GAS protein was separated on a 7.5% SDS-polyacrylamide gel electrophoresis (PAGE) and transferred to PVDF membrane. MHC was detected with mouse monoclonal primary antibody against all isoforms of MHC (MF20, Developmental Studies Hybridoma Bank, 0.06 µg/mL) and iodinated goat anti-mouse (GAM) secondary antibody (Perkins Elmer 1:20 000). An iodinated secondary antibody was found to minimize non specific signals. The radioactive signal was detected using a phosphoimager. Tropomyosin was detected by mouse monoclonal primary antibody against tropomyosin (CH1, 0.5 µg/mL) and GAM secondary antibody conjugated to horse radish peroxidase (HRP) (1:10 000). Chemiluminescent signal was produced by ECL Plus (Amersham) and signals recorded by a BioRad VersaDoc imager.

To quantify of Poly-ADP-Ribose-Polymerase (PARP) and caspase-3, equal fractions of GAS lysate were separated on 7.5% and 15% SDS-PAGE gel respectively. Gels were transferred to a PVDF membrane. PARP was detected by

a rabbit polyclonal antibody (Anti-PARP LaRoche™, 1:2000) and goat-anti-rabbit (GAR)-HRP secondary antibody (New England Bio Labs 1:10 000). Caspase-3 was detected by mouse monoclonal antibody against caspase-3 (Cell Signalling™ 1:1000) and GAM-HRP secondary antibody. For both PARP and caspase-3, chemiluminescent signal was produced using ECL Plus and this was detected on an x-ray film.

All western blot images were quantitated by volumetric analysis with Quantity One 1 D analysis™ from BioRad. All reported results are shown as means ± standard errors. Tropomyosin and MHC content are reported in arbitrary units assigned by chemiluminescence signal intensity. Levels of fragmented PARP and caspase-3 in GAS muscle were expressed as a percentage of total PARP or caspase 3 respectively .

2.4 Morphometry

Serial sections of frozen GAS (7 µm) were obtained from USP19 KO or WT mice on a cryostat. Each section was stained by immunohistochemistry for MHC fibers. Tissue was stained with mouse monoclonal antibodies (American Type Culture Collection), - anti-BAD5 for type I fibers, anti-SC71 for type IIa fibers or anti-BFF3 for type IIb fibers and detected with IgG coupled to biotin and bound to streptavidin (Vector labs) in the presence of HRP. The IgG binds specifically to the gamma chain of the primary antibody.

Stained sections were digitally photographed at 40x magnification, at the complex zone of the GAS (contains all four fiber types). Serial sections, each stained for a different fiber type were aligned to permit fiber type identification of all fibers. Quantitation of the area of 200 fibers was done using Quantity One 1 D analysis™ from BioRad. All results are reported as means ± standard errors.

2.5 Statistical Analyses

Student's t-tests were applied to determine p values when comparing means. Paired t-tests were used to compare data from innervated and denervated muscles. Unpaired t-tests were used to compare data from WT and KO samples.

III RESULTS:

3.1 Gastrocnemius of USP19 KO mice has higher muscle mass compared to wild type littermates

To evaluate the role of USP19, mice heterozygous for USP19 gene inactivation were bred together to generate wild type (WT) and homozygous null (KO) mice. Overall appearance, behaviour and body weights were similar in both WT and USP19 KO mice in males, aged 9-11 months and females, aged 4-8 months (Tables 2 & 3). The hindlimb muscles, tibialis anterior (TA) and GAS of males, aged 9 to 11 months, and females, aged 4 to 8 months, were weighed for both USP19 KO and WT mice. GAS muscles of male USP19 KO mice were ~6% heavier than those of WT littermates. This was a slight, but significant difference between KO and WT GAS muscle (Table 2). There was a trend towards similar difference in mass in the TA muscle (KO TA 10% heavier than WT) (Table 2). Female KO mice had slightly heavier GAS muscles than WT mice, but they were not statistically different (Table 3).

To explore if the effects of USP19 loss were specific to muscle, I determined the weights of other major organs, where USP19 is known to be expressed. Since muscle mass was higher but overall body weight was similar between genotypes, other organs could be slightly smaller. We therefore harvested and weighed major tissues. The kidney and liver of KO mice had similar mass to WT littermates. Interestingly the heart was significantly smaller in USP19 KO mice than WT mice (Table 4). Since these were female mice, we verified testis size in males and found a significant reduction in testis mass that corresponds to a severe defect in fertility (fertility data not show) (Table 4).

	Tibialis Anterior			
	WT		KO	P value
Control mass (mg)	52.9	± 2.4	58.8 ± 2.3	<0.1
Denervated mass (mg)	38.5	± 1.4	48.3 ± 1.7	<0.001
Mass lost (mg)	14.4	± 1.6	10.5 ± 0.8	<0.02
% Mass lost	26.9	± 2.1	17.8 ± 0.8	<0.004
	Gastrocnemius			
	WT		KO	P value
Control mass (mg)	152	± 4.5	167 ± 4.9	< 0.05
Denervated mass (mg)	96	± 4.4	122 ± 4.2	<0.005
Mass lost (mg)	56	± 4.6	45 ± 4.8	<0.05
% Mass lost	36.6	± 2.8	26.8 ± 2.5	<0.02
	WT		KO	P value
Body Weight (g)	34.55	± 2.0	34.96 ± 1.2	NS

Table 2: Male USP19 KO mice lose less mass than WT mice in TA and GAS muscles following sectioning of the sciatic nerve. Male mice, age 9-11 months, underwent sectioning of the sciatic nerve in one hindlimb (Den) and a sham (Control) operation in the contra-lateral limb. Two weeks later the muscles were isolated and weighed (N= 5KO, 6WT). (The percent of muscle mass lost = mg mass lost/Control weight * 100).

3.2 Male USP19 knockout mice lose less muscle mass after denervation than wild type littermates

To determine the skeletal muscle changes resulting from USP19 disruption in response to muscle wasting stimuli, USP19 WT and KO mice, ages 9 to 11 months, were denervated (den) unilaterally by sectioning the sciatic nerve in one leg, while the contra-lateral leg served as a control (Table 2). Denervation for a period of 14 days is known to cause severe wasting in hindlimb muscles on the same side as the severed nerve; in particular, TA and GAS are two mixed-muscles which experience wasting. As previously reported, such denervation in normal mice results in muscle wasting and causes considerably lower muscle mass in the TA and GAS (Table 2). Interestingly, KO mice showed less wasting than WT littermates in both the TA and the GAS when wasting was calculated, either as absolute mass lost or as a percentage of muscle mass lost. The inactivation of USP19 in mice led to approximately 30% muscle sparing of denervation induced atrophy.

3.3 USP19 KO mice sparing is not gender specific

To determine if muscle sparing in response to denervation was gender dependant, the same denervation experiment was performed in female WT and KO mice. As expected, WT mice lost a significant portion of TA and GAS muscle mass during denervation (Table 3). Similar to males, the percentage of muscle mass lost in KO GAS and TA was significantly less than the loss seen in WT GAS and TA. The absolute mass lost in GAS and TA of females, was significantly lower in KO mice, as was previously seen in males. Since both experiments showed a dramatic sparing of GAS muscle mass, the muscle content in GAS was analyzed biochemically.

	Tibialis Anterior		
	WT	KO	P value
Control mass (mg)	42.8 ± 3.1	43.9 ± 1.3	NS
Denervated mass (mg)	29.5 ± 3.3	37.3 ± 0.9	<0.1
Mass lost (mg)	13.3 ± 1.7	8.5 ± 2.2	< 0.04
% Mass lost	32 ± 4.4	15 ± 2.6	<0.025
	Gastrocnemius		
	WT	KO	P value
Control mass (mg)	132 ± 9.2	142 ± 8.3	NS
Denervated mass (mg)	75.0 ± 7.5	106 ± 7.6	<0.025
Mass lost (mg)	56.9 ± 3.7	30.7 ± 7.5	<0.003
% Mass lost	44 ± 2.5	25 ± 4.4	<0.005
	WT	KO	P value
Body Weight (g)	33.0 ± 4.4	35.7 ± 5.3	NS

Table 3: Female USP19 KO mice lose less mass than WT mice in TA and GAS muscles following sectioning of the sciatic nerve. Female mice, age 4-8 months, underwent sectioning of the sciatic nerve in one hindlimb (Den) and sham (Control) operations in the contra-lateral limb. Two weeks later the muscles were isolated and weighed (N= 4KO, 5WT). (The percent of muscle mass lost = mg mass lost/Control weight * 100).

Males	WT	KO	P value
Testis Mass (mg)	94 ± 4.8	58.5 ± 9.9	<0.004

Females	WT	KO	P value
Heart Mass (mg)	166 ± 12.6	124 ± 9.6	< 0.03
Liver Mass (g)	1.37 ± 0.13	1.17 ± 0.17	<0.3
Kidney (mg)	195 ± 19.9	147 ± 13.9	<0.07

Table 4: Mass of mouse organs in male and female USP19 KO and WT mice.
(Males: N = 5 KO, 6 WT; Females: N = 4KO, 5WT)

3.4 USP19 KO mice lose less muscle protein content than WT littermates

Since muscle is composed predominantly of water and protein it was important to determine if mass differences between USP19 KO and WT mice were due to differences in protein content in skeletal muscle. The GAS was used to measure cellular protein content. Since the age and body weights of WT and KO male mice were more closely paired than those of the female mice, biochemical analyses were performed on samples from the study with males. The results showed that KO muscle had a higher protein content than WT muscle. As previously demonstrated, denervation induced a significant protein loss in WT muscle. Consistent with difference in muscle mass, protein content in KO muscle was 33% greater than that of WT muscle post-denervation (Fig 4A). Control muscles from the KO mice were marginally higher in protein content than control muscles from WT mice but this difference was not significant. The total loss of cellular protein as a result of denervation was comparable between WT and KO mice (WT= 3.85 mg; KO = 3.99 mg).

3.5 USP19 KO mice have higher myofibrillar protein levels after denervation

Previous studies in L6 myotubes show that depletion of USP19 results in an increase in levels of myofibrillar protein. Silencing USP19 in L6 myotubes is shown to significantly increase many myofibrillar proteins including MHC and tropomyosin. The greatest increase is seen in tropomyosin⁵¹. To determine if similar effects occurred *in vivo*, the content of tropomyosin and MHC, in the GAS muscle homogenates, was measured by Western blot analysis (Fig 5A). KO mice when compared to WT mice showed a trend towards higher levels of tropomyosin but this difference was not statistically significant. Average MHC levels were similar in KO and WT mice. As expected, denervation of WT muscle caused a significant decrease in tropomyosin and MHC content (Fig 5B). Denervation of KO muscle did not cause a decrease in MHC (Fig 5C). However, tropomyosin levels were significantly higher in KO mice after denervation when compared to denervated WT littermates. Consistent with this, MHC levels showed a similar

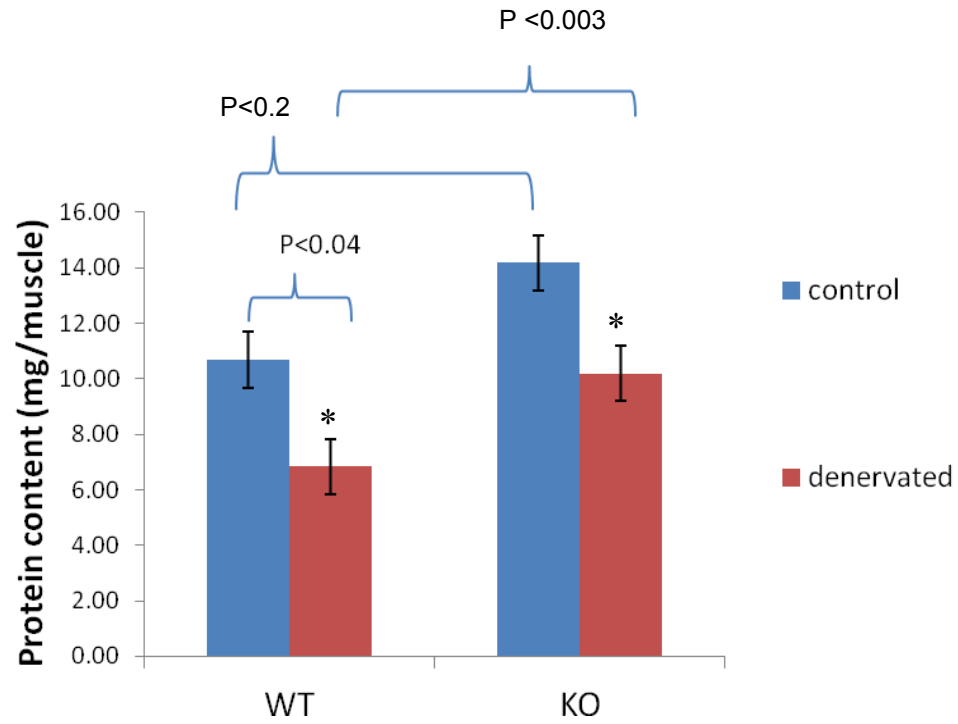


Figure 4. Protein content is higher in GAS muscle in male USP19 KO mice than WT mice following sectioning of the sciatic nerve. Control was sham operated. Protein content per GAS muscle (N = 4 KO, 5 WT).

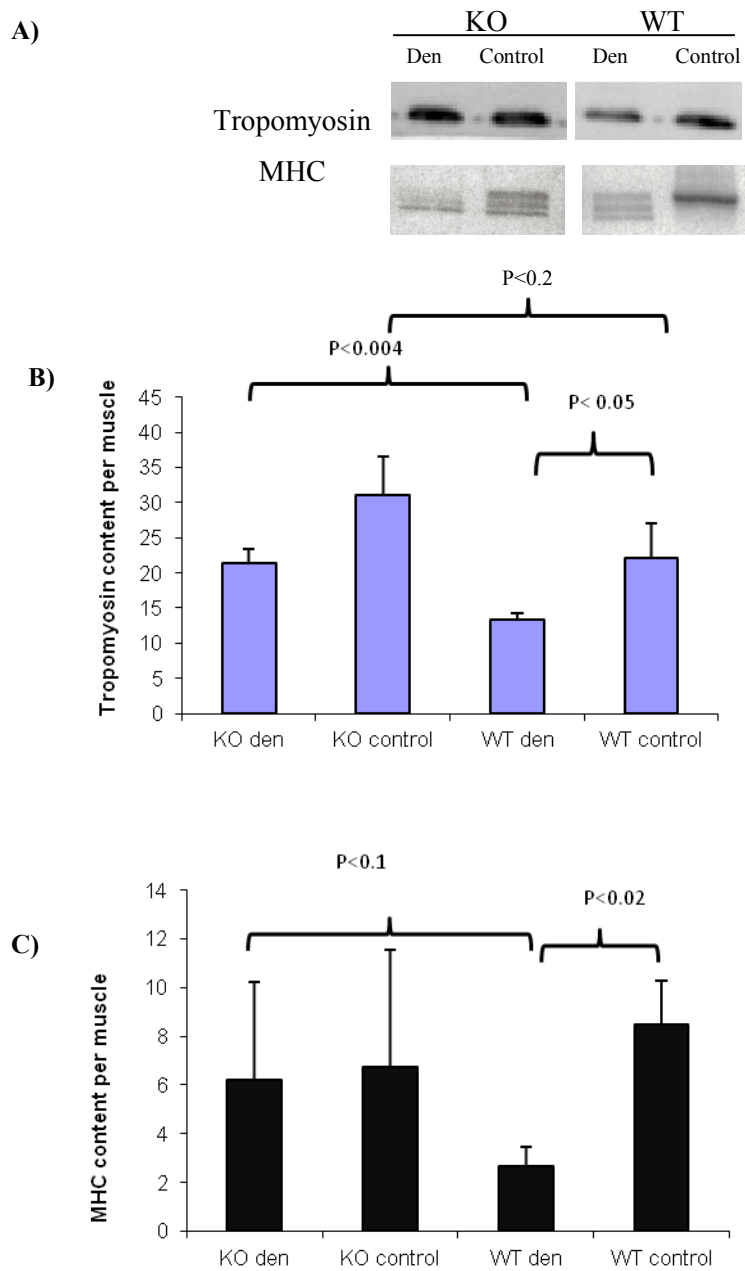


Figure 5: Tropomyosin and MHC protein is higher in GAS muscles of USP19 KO mice compared to WT mice 14 days after severing the sciatic nerve. (A) Representative Western blots of tropomyosin and MHC in GAS homogenate. Den: Denervated limb; Control: Sham operated limb. Denervation 14 days. Quantitation of **(B)** tropomyosin and **(C)** MHC (IIa, IIx/d and IIb isoforms detected) (N= 4 KO, 5 WT).

trend, being slightly higher in USP19 KO muscle than WT muscle after this catabolic stimulus (Fig 5C). Taken together, this data demonstrates that USP19 is required for the down regulation of myofibrillar protein content in skeletal muscle, after loss of muscle innervations

3.6 USP19 KO muscle have more muscle fibers than WT mice

To determine if the sparing of muscle and protein seen in KO mice after denervation was due to changes in fiber volume, I measured the fiber cross sectional area (CSA) in the GAS complex zone of female USP19 KO and WT mice. The complex zone contains all four fiber types (I, IIA, IIB, IIX). The average CSA of all four fiber types in the complex zone of the GAS was slightly larger in KO females than in WT females (KO 6% larger than WT) (Fig 7A). The average CSA in KO was $166 \text{ um}^2 \pm 3.68$ while WT CSA was only $155 \text{ um}^2 \pm 3.34$. After denervation, the CSA of WT muscles were significantly less than that of KO muscles (WT = $113 \text{ um}^2 \pm 1.78$ vs KO = $119 \text{ um}^2 \pm 1.93$ $p < 0.01$). However, despite this significant difference between WT and KO denervated samples, volume differences could only account for 5% of sparing (assuming both muscles contained the same number of fibers after denervation). Analysis of the GAS from male WT and KO mice provided similar results (data not shown). However, sparing of muscle mass and protein content in KO was approximately 30% (Table 2 & 3; Fig 4). The data implies that USP19 KO mice must have more muscle fibers than WT mice after denervation, to account for the 30% higher overall muscle mass and protein content.

Analysis of the fiber distributions of the CSA did not show a remarkable shift between the mode of KO as compared to the mode of WT fibers. The mice most closely paired in age and weight have been shown as representative samples (Fig 7). Interestingly, the number of fibers greater than the mode is higher in KO mice (155 fibers per 200) than in the WT mice (148 fibers per 200) even though the modes were similar in both genotypes (Fig 7). As expected, denervation decreased the CSA for both KO and WT muscle when compared to controls.

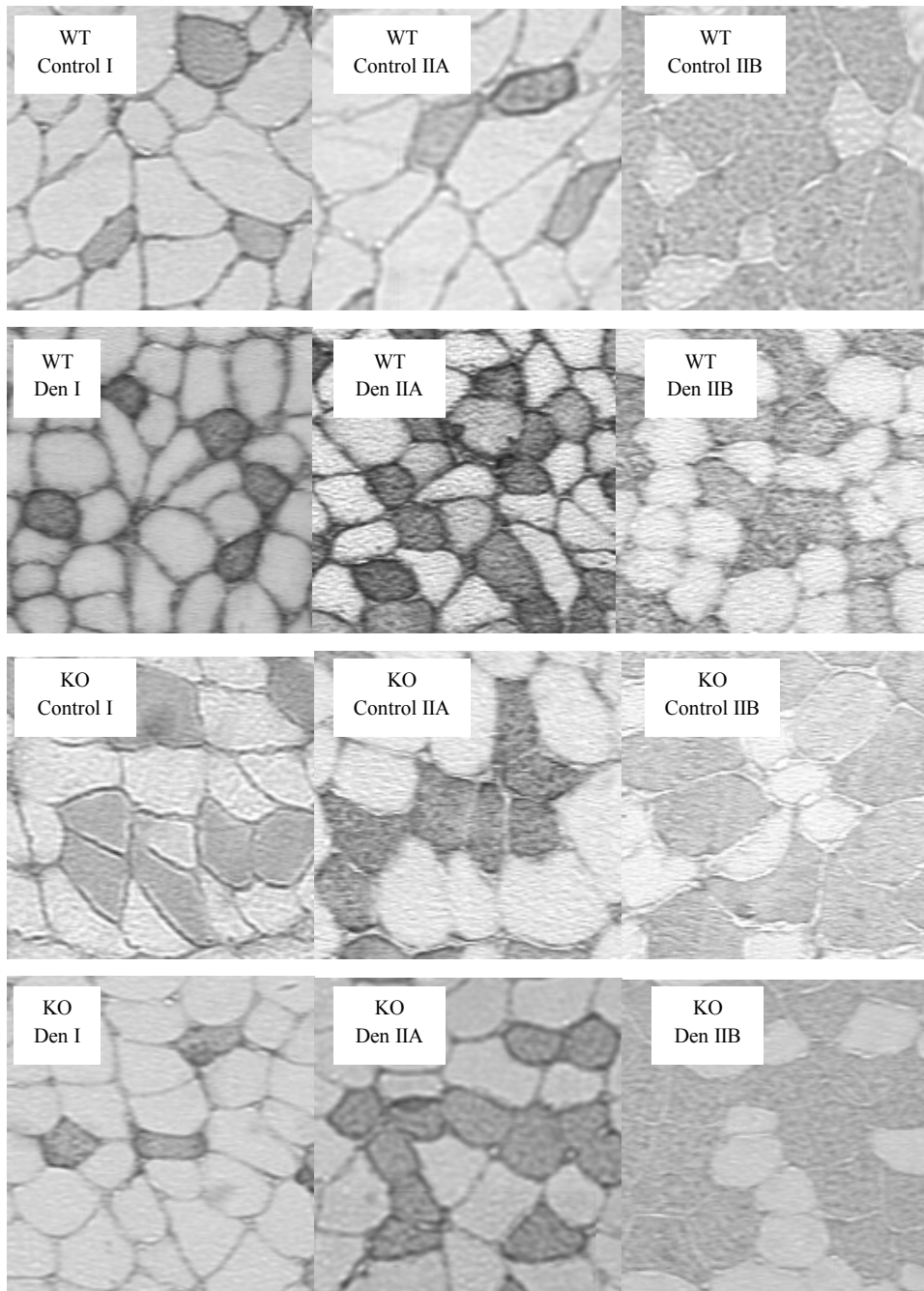


Figure 6: Light microscopy images of immunohistochemical stain of type I, IIA and IIB MHC in WT and KO GAS of mice severed at the sciatic nerve. Representative samples taken at 40x magnification from serial sections (7 μ m)

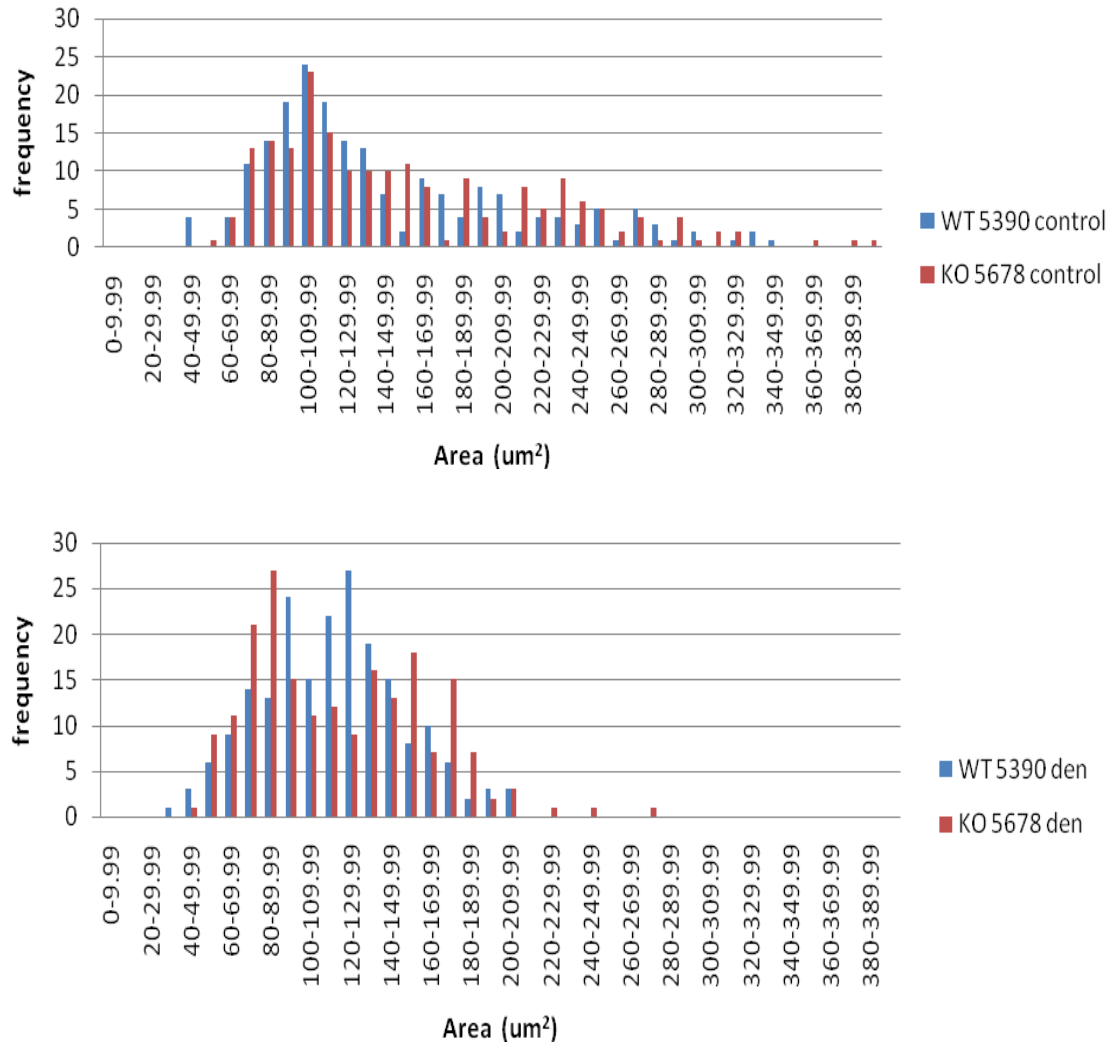


Figure 7: Distribution of fiber CSA in GAS of WT and KO mice severed at the sciatic nerve. Frequency refers to the occurrence of fibers within that CSA in a population of 200 fibers.

What is notable, the mode CSA was lower in KO mice (occurring between 80-89 μm^2) than WT mice (occurring 90-99 μm^2) however, KO muscle had more fibers above the mode (137 fibers) than WT mice (66fibers). To explain this difference between mode of CSA and muscle mass, I explored whether the effect of USP19 inactivation preferentially spares the CSA of specific fiber types by measuring the average CSA for each fiber type in WT and KO GAS muscle (Fig 8B). Serial sections of GAS were stained for either MHC isoform I, IIA or IIB (Fig 6). Unlabeled fibers are MHC IId/x and designated type IIX. Most of the fiber types (IIA, IIB and IIX) were comparable in WT and KO mice. However, the CSA of type I fibers in KO mice were larger than type I fibers in WT mice ($P<0.0001$). Since type I fibers account for approximately 6% of all fibers in the GAS of C57bl/6J mice and these fibers are the smallest of all fibers present in fast-twitch muscle, their higher CSA (thus higher volume) has a negligible effect on total muscle mass¹³. Analysis of CSA of type IIB fibers revealed that these fibers are larger in KO than WT (253 μm^2 vs 229 μm^2) representing 10% hypertrophy. Since, IIB fibers account for 55% of all GAS fibers and these fibers have the largest CSA in fast-twitch muscle, type IIB fibers may be responsible for the slightly larger mass of KO muscles compared to WT muscle (Table 2)¹³. taken from one female WT and USP19 KO mouse. Control: Sham operated muscle; Den: muscle denervated limb. IIX fibers are those not stained by any of the three antibodies (anti-I, IIA or IIB).

After denervation the IIB KO fibers are larger than IIB WT fibers (150 μm^2 vs 127 μm^2 ; $P<0.0001$), showing a 4% sparing of wasting which is similar to the 5% sparing seen in the average CSA when all fibers are considered. There is also 2% sparing in CSA in KO IIX fibers (den KO =147 μm^2 ; den WT = 131 μm^2 ; $P<0.005$), representing approximately 12% of GAS fibers population in C57bl/6 mice¹³. Since, blocks of GAS tissue may have been sectioned at slightly different angles to one another, such changes could influence the CSA of the fibers. To account for these differences, the fiber type data was normalized to IIA fibers, which show the least variance between groups (Fig 8C). The normalized data reflects similar trends seen in the raw data, indicating that deviations in sectioning

were probably negligible. Taken together, the mild but significant effects of sparing on the type IIB and IIX fibers CSA do not account for the one third of muscle and protein sparing seen in KOs.

3.7 USP19 KO muscle undergoes less apoptosis during denervation

To better understand the mechanisms by which mice lacking USP19 were spared from denervation induced wasting seen in WT littermates, we examined the DNA content of GAS muscles from male mice. Assuming that multinucleated myofibers within a given muscle contain approximately the same number of nuclei, cell number was approximated by quantification of DNA. Although DNA content in the control muscles were similar between WT and KO groups, although it should be noted that KOs GAS had slightly more DNA content than WT GAS muscle, correlating with the heavier muscle mass previously observed in KO GAS prior to treatment (Fig 8A).

Denervation stimuli caused DNA loss in WT mice (Fig 8A) consistent with evidence previously reported that denervation-induced wasting triggers apoptotic signalling cascades⁵⁴. However, KO mice showed less DNA loss than WT after denervation, suggesting that less apoptosis was occurring. To explore this further, two markers of apoptosis were examined, Caspase-3 cleavage and PARP cleavage. There was a trend towards increased Caspase-3 cleavage after denervation in WT GAS but no alteration in the percentage of cleaved Caspase-3 for KO GAS groups (Fig 8B).

Similarly, there was increased PARP cleavage in the denervated muscle WT mice compared to WT controls, but no difference in the percentage of PARP cleavage in control versus denervated KO GAS (Fig 8C). Interestingly, after denervation PARP cleavage was significantly less in KO GAS than in WT GAS, confirming that USP19 was required for an increase in apoptotic signalling markers after this wasting stimulus was applied. Take together, Caspase-3 and PARP data suggest that USP19 KO skeletal muscle is less susceptible to cell death after loss of innervation.

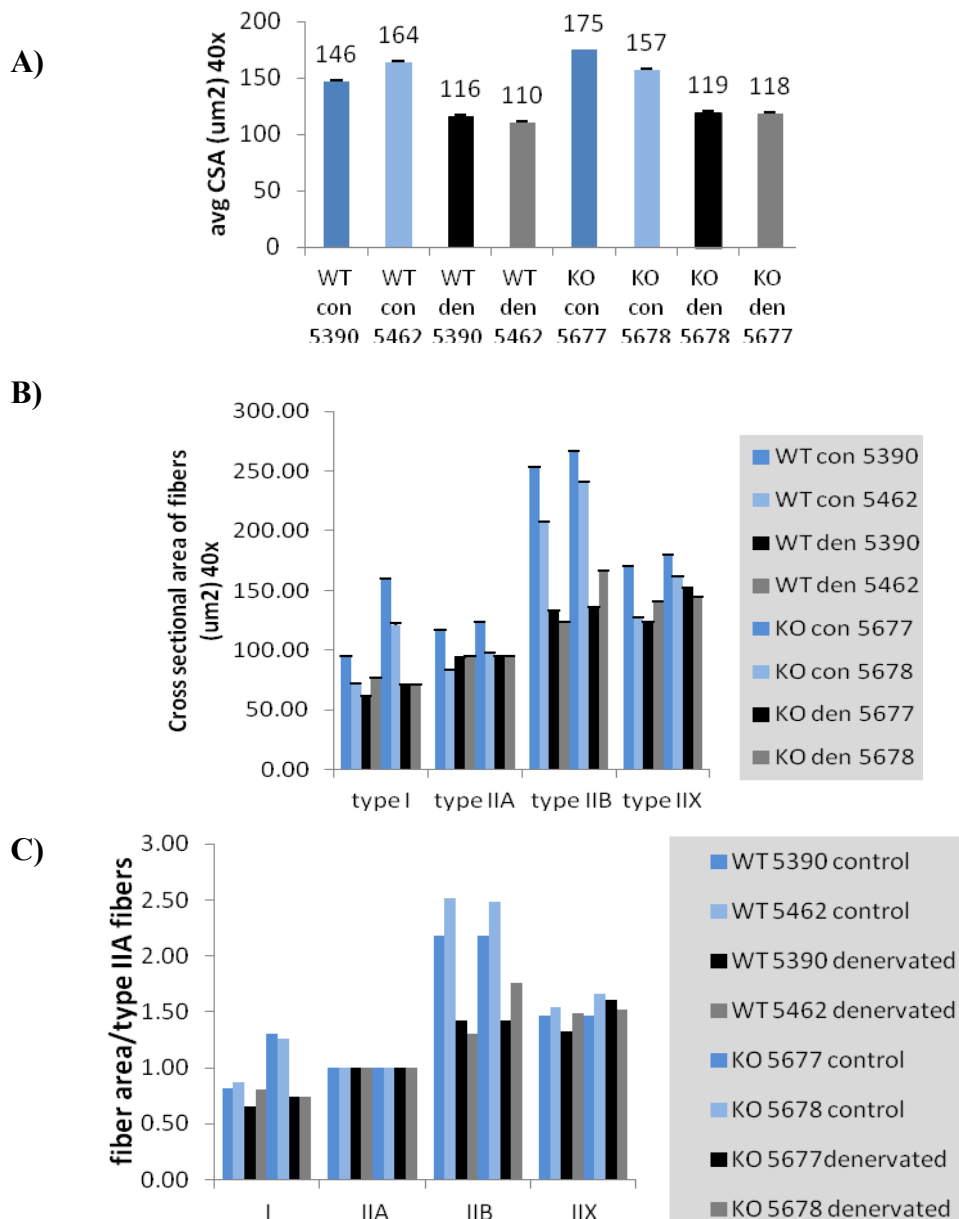
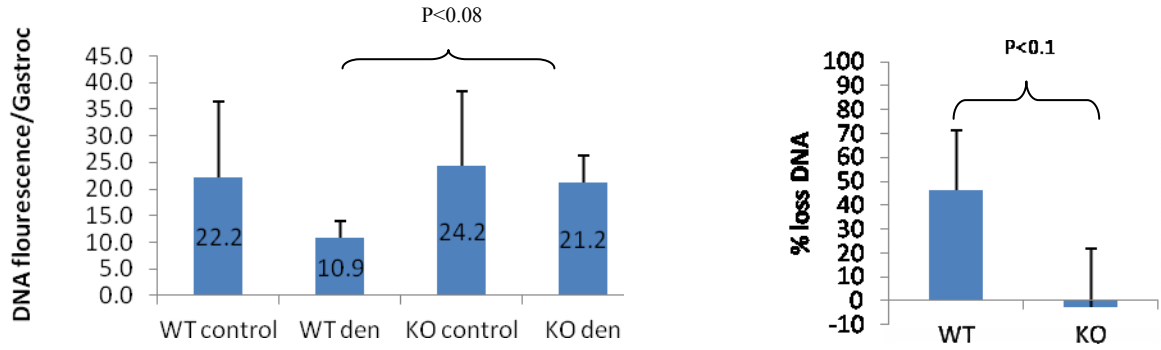
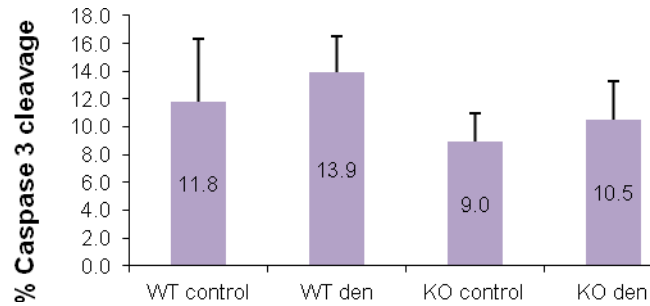


Figure 8 : The Cross sectional Area of Gastrocnemius fibers in WT and USP19 KO mice post denervation. A. Average cross sectional area of fibers in the complex zone of GAS. Numerical averages are indicated above the bar (Shown are means \pm SE; N=200 fibers) (denervated WT vs KO P<0.015). **B.** Cross sectional area of each fiber type in the complex zone identified by immunohistochemistry. The error bars are so small they are invisible using the current scale (Shown are means \pm SE; N>20 per fiber type) **C.** CSA of each fiber type normalized to type IIA fibers.

A)



B)



C)

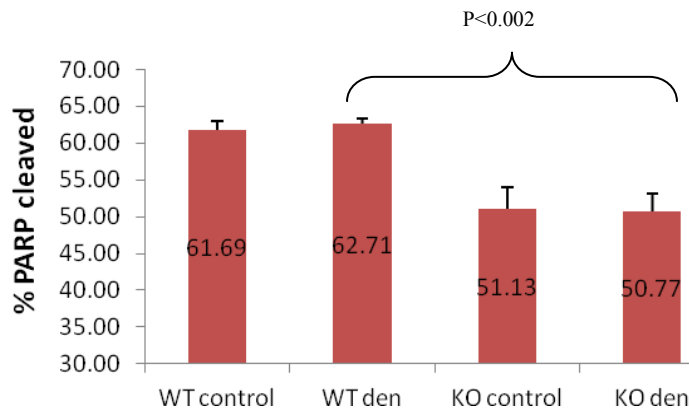


Figure 9: Male USP19 KO mice lose less DNA content and show less PARP cleavage than WT mice when undergoing severing of the sciatic nerve. (A) DNA content and percent loss of DNA after denervation (B) Percentage of Caspase-3 cleavage (fragment/full+fragment) (C) PARP cleavage (fragment/full+fragment) as measured in GAS homogenates male mice (N = 4 KO, 5 WT).

TUNEL staining was attempted on muscle sections; however, we did not observe any staining in either WT or KO muscles. One possible explanation is that skeletal muscle fibers are multi-nucleated and may contain normal and apoptotic nuclei simultaneously. In addition, Broisov and Carlson reported non-classical apoptosis in muscle fibers, characterized by abnormal chromatin structure in the nuclei in the EDL, TA and soleus of rats without co-localization of TUNEL stain.⁵⁵ Another possible explanation is that positive TUNEL staining may be time dependant and occurred prior to the 14 day time point after denervation that we examined. Broisov and Carlson also report that after skeletal muscle loses neural stimulation the loss of muscle fibers diminishes over time.

IV DISCUSSION:

In this thesis, I have demonstrated for the first time an essential role of USP19 *in vivo* in modulating skeletal muscle growth and skeletal muscle response to wasting. Deletion of USP19 in mice may lead to skeletal muscle hypertrophy since some skeletal muscles in KO mice are larger than those in WT littermates. In particular, KO GAS mass was significantly heavier than WT GAS mass in males and had slightly higher protein content and tropomyosin content. KO TA mass showed a trend towards hypertrophy as compared to WT TA mass. Therefore, USP19 KO mice differ in their skeletal muscle development from E3 ligase KO mice, MuRF1^{-/-} or MAFbx^{-/-} mice, which reportedly have similar skeletal muscle mass under normal conditions⁴. The hypertrophy seen in USP19 KO mice was mild and more evident in the mice age 9-11 months than in the mice age 4-8 months, suggesting that this hypertrophy is progressive over time, although a sex effect cannot be dismissed. This suggests that USP19 plays an important role in skeletal muscle.

The effects of USP19 on myofibrillar protein content is likely indirect as loss of USP19 deubiquitinating activity would be predicted to destabilize its substrates. Instead, USP19 may alter the transcription of the myofibrillar proteins. Previously, our laboratory reported that depletion of USP19 in rat myotubes stimulates myogenin transcription⁵¹. This *in vitro* data raise the possibility that USP19 may regulate fiber number during skeletal muscle development through the modulation of myogenin. Therefore, it will be of interest to determine whether deletion of USP19 in the mouse results in increased myogenin expression and increased fiber number during skeletal muscle growth and development, contributing to the hypertrophy observed in GAS muscle.

In the female mice, liver and kidney masses were comparable between KO and WT mice. Interestingly, female KO mice had significantly smaller hearts, but showed no evidence for any gross functional defect. Male KO mice had significantly smaller testes accompanied by reduced fertility (data not shown). The associated decrease in testis size suggests an essential role for USP19 in

spermatogenesis. Interestingly, this tissue mass decrease is inversely correlated to the level of USP19 mRNA measured in rats, where USP19 is highly expressed in testes and heart and less expressed in liver and kidney⁵⁰.

My thesis demonstrates that USP19 deletion spares muscle mass from severe denervation-induced wasting by reducing mass and protein loss. Moreover, this effect of muscle sparing is not gender specific. The extent of muscle mass spared between WT and KO groups was ~30% which is similar to the level of sparing previously reported in MuRF1^{-/-} and MAFbx^{-/-} mice⁴. In addition, our lab has recently observed that dexamethasone treatment or food deprivation also induces less muscle wasting in USP19 KO mice than in WT mice (data not shown). Therefore, USP19 is required for the full wasting response to catabolic stimuli and inhibition of USP19 may be able to inhibit muscle atrophy.

The mechanism by which sparing occurs remains to be defined. The data presented in my thesis indicates that the increased muscle mass is associated with increased myofibrillar protein content. This suggests that muscle strength should be better in the USP19 KO mice, but this remains to be tested directly. Interestingly, in contrast to what has been observed with MuRF1^{-/-} and MAFbx^{-/-} mice, the reduced wasting does not appear to be simply due to reduced fiber atrophy. Cross sectional fiber area was only 5% larger in denervated KO muscle as compare to denervated WT muscle and cannot account for the 30% difference in muscle mass. Furthermore, quantification of DNA content in GAS muscles revealed more DNA content in USP19 KO muscle than in WT mice after denervation stimulus was applied. This preliminary evidence raised the interesting possibility that USP19 KO mice undergo less myofiber apoptosis as a consequence of denervation than WT mice. In support of this my preliminary evidence showed that there was reduced Caspase-3 and PARP cleavage in USP19 KO mice as compared to WT mice in response to denervation stimuli. Thus USP19 appears to regulate muscle size through mechanisms distinct from that of the E3 ligases, MAFbx and MuRF1, which primarily affect fiber size. Taken together, my thesis reports that USP19 has a novel mechanism for modulating muscle fiber size.

To better understand the mechanism by which USP19 influences fiber number several parameters should be explored: the muscle fiber number should be measured at various points during development and wasting; markers of apoptosis should be verified during a time course after denervation; molecular changes such as increased actin, troponin and myogenin observed in skeletal muscle cells *in vitro* should be verified in USP19 KO muscle; and USP19 substrates should be identified. Studies of denervation-induced atrophy report evidence that cell death and disorganization of the sarcomere occurs when skeletal muscle loses neural stimulus (Pellegrin), (rev in ⁵⁶). Therefore, electron microscopic structure of USP19 KO muscle should also be evaluated.

In summary, USP19 deletion provides protection against muscle wasting, induced by various catabolic stimuli. This muscle sparing appears to occur via a novel mechanism, whereby USP19 deletion promotes skeletal fiber survival after loss of neuronal stimulation. USP19 could potentially be targeted for the treatment of wasting from various catabolic disorders including where loss of neural stimulation causes disease progression, such as stroke, amyotrophic lateral sclerosis and peripheral neuropathies.

REFERENCES:

- ¹ Mitch W.E., and Goldberg A.L. *Mechanisms of Muscle Wasting — The Role of the Ubiquitin–Proteasome Pathway*. NE JM. 1996; **335**:1897-1905.
- ² Larsson L. *Experimental animal models of muscle wasting in intensive care unit patients*. Crit. Care Med. 2007; **35**: 484-7.
- ³ Goldberg A.L. *Protein Turnover in Skeletal Muscle: Effects of Denervation and Cortisone on Protein Catabolism in Skeletal Muscle*. The Journal of Biological Chemistry. 1969; **244**: 3223-3229
- ⁴ Bodine S.C., Latres E., Baumhueter S., Lai V.K., Nunez L., Clarke B.A., Poueymirou W.T., Panaro F.J., Na E., Dharmarajan K., Pan Z.Q., Valenzuela D.M., DeChiara T.M., Stitt T.N., Yancopoulos G.D., and Glass D.J. *Identification of ubiquitin ligases required for skeletal muscle atrophy*. Science. 2001; **294**:1704-1708
- ⁵ Pellegrin C., and Franzini C.. *An electron microscope study of denervation atrophy in red and white skeletal muscle fiber*. JBC 1963; **17** : 327-233.
- ⁶ Siu P.M., and Alway S.E.. *Mitochondria associated apoptotic signalling in denervated rat skeletal muscle*. J. Physio. 2005; **561**; 309-323
- ⁷ Kuang, S., Kuroda K., Le Grand, F. and Rudnicki M.A. *Asymmetric Self-Renewal and Commitment of Satellite Stem Cells in Muscle*. Cell. 2007; **129**: 999–1010
- ⁸ Birchmeier, C., and Brohmann, H. *Genes that control the development of migrating muscle precursor cells*. Curr. Opin. Cell Biol. 2000; **12**: 725–730
- ⁹ Sabourin, L.A., Rudnicki, M.A. *The molecular regulation of myogenesis*. Clin. Genet. 2000; **57**: 16–25
- ¹⁰ Sutherland C.J., Esser K.A., Elsom V.L., Gordon M.L., and Hardeman, E.C. *Identification of a Program of Contractile Protein Gene Expression Initiated Upon Skeletal Muscle Differentiation*. Developmental Dynamics. 1993; **196**: 25-36.
- ¹¹ Rethinasamy P., Muthuchamy M., Hewett T., Boivin G., Wolska B.M., Evans C., Solaro R.J., Wieczorek D.F. *Molecular and Physiological Effects of -Tropomyosin Ablation in the Mouse*. *Circulation Research*. 82:116-123 (1998)
- ¹² Stienen G. J. M., Kiers J. L., Bottinelli R. and C. Reggiani. *Myofibrillar ATPase activity in skinned human skeletal muscle fibers: fiber type and temperature dependence*. Journal of Physio. 1996; **493**: 299-307
- ¹³ Augusto V., Padovani R.C. and Campos G,E.R. *Skeletal Muscle Fiber Types In C57bl6j Mice*. Braz. J. morphol. Sci. 2004; **21**: 89-94
- ¹⁴ Burkholder T.J., Fingado B., Baron S., and Lieber R.L. *Relationship Between Muscle Fiber Types and Sizes and Muscle Architectural Properties in the Mouse Hindlimb*. Journal Of Morphology. 1994; **221**:177-190.
- ¹⁵ Bobinac, D. Malnar-Deragojevic D., Soic-Vranic T., and Jerkovic R. *Muscle fiber type*

composition and morphometric properties of denervated rat extensor digitorum longus muscle. Croat. Med. J. 2000; **41**:294-7.

¹⁶ Ventadour S., and Attaix D. Mechanisms of skeletal muscle atrophy. *Curr Opin Rheumatol.* 2006; **18**:631-635.

¹⁷ Price S.R., Bailey J.L., Wang X., Jurkovitz C., England B.K., Ding X., Phillips L.S. and Mitch W.E. *Muscle wasting in insulinopenic rats results from activation of the ATP-dependent, ubiquitin-proteasome proteolytic pathway by a mechanism including gene transcription.* J. Clin. Invest. 1996; **98**: 1703-1708.

¹⁸ Wing S.S. *Control of ubiquitination in skeletal muscle wasting.* The International Journal of Biochemistry & Cell Biology. 2005; **37**: 2075–2087.

¹⁹ Spencera J.A., Eliazerb S., Ilaria R.L., Richardson J.A., and Olsons E.N. *Regulation of Microtubule Dynamics and Myogenic Differentiation by Murf, a Striated Muscle Ring-Finger Protein.* JCB. 2000; **150**; 771-784.

²⁰ Sun Y. *Targeting E3 ubiquitin ligases for cancer therapy.* Cancer Biol Ther. **2**: 623-9 (2003).

²¹ You, J. and Pickart C.M., *A HECT Domain E3 Enzyme Assembles Novel Polyubiquitin Chains.* JBC. 2001; **276**: 19871-19878.

²² Ho MS, Ou C, Chan YR, Chien CT, Pi H. *The utility F-box for protein destruction.* Cell Mol. Life Sci. 2008; **65**:1977-2000.

²³ Tintignac LA, Lagirand J, Batonnet S, Sirri V, Leibovitch MP, Leibovitch SA. *Degradation of MyoD mediated by the SCF (MAFbx) ubiquitin ligase.* J Biol Chem. 2004; **280**:2847-56.

²⁴ Xu, P., Duong, D.M., Seyfried, N.T., Cheng, D., Xie, Y., Robert, J., Rush, J., Hochstrasser, M., Finley, D., and Peng, J. *Quantitative Proteomics Reveals the Function of Unconventional Ubiquitin Chains in proteasomal Degradation.* Cell. 2009; **137**: 133–145.

²⁵ Taillandier D., Combaret L., Pouch M.N, Samuels S.E., Be'chet D. and Attaix D. *The role of ubiquitin-proteasome-dependent proteolysis in the remodelling of skeletal muscle.* Proceedings of the Nutrition Society. 2004; **63**:357–361.

²⁶ Ventii K.H. and Wilkinson K.D. *Protein Partners of Deubiquitinating Enzymes.* Biochem. J. 2008; **414**: 161-175.

²⁷ Pickart C.M. *Ubiquitin in chains.* Trends in Biochemical Sciences. 2000; **25**: 11 544-548

²⁸ Tawa N.E., Goldberg A.L. *Protein and amino acid metabolism in muscle.* Myology: basic and clinical. 2nd ed. New York: McGraw-Hill, (1994) 683-707

²⁹ Booth F. W., and D. S. Criswell. *Molecular Events Underlying Skeletal Muscle Atrophy and the Development of Effective Countermeasure.* Int J Sports Med 1997; **18**: S265-S269

³⁰ Fielitz J., Kim M.S., Shelton J.M., Latif S., Spencer J.A., Glass D.J., Richardson J.A., Bassel-Duby R., Olson E.N. *Myosin accumulation and striated muscle myopathy result from the loss of muscle RING finger 1 and 3.* J Clin Invest. 2007; **117**:2486-95.

³¹ Bodine S.C., Latres E., Baumhueter S., Lai V.K., Nunez L., Clarke B.A., Poueymirou W.T.,

-
- Panaro F.J., Na E. and Dharmarajan K. *Identification of Ubiquitin Ligases Required for Skeletal Muscle Atrophy*. Science. 2001; **294**: 1704–1708
- ³² Lagirand-Cantaloube J., Cornille K., Csibi A., Batonnet-Pichon S., Leibovitch M.P., and Leibovitch S.A. *Inhibition of Atrogin-1/MAFbx Mediated MyoD Proteolysis Prevents Skeletal Muscle Atrophy In Vivo*. PLoS ONE. 2009; **4**: e4973-78
- ³³ Khala J., Hinea A.V., Fearonb K.C.H., Dejongc C.H.C., Tisdalea M.J. *Increased expression of proteasome subunits in skeletal muscle of cancer patients with weight loss*. IJBCB. 2005; **37**:2196–2206
- ³⁴ Tiao G., Hobler S., Wang J.J., Meyer T.A., Luchette F.A., Fischer J.E., and Hasselgren P.O.. *Sepsis is associated with increased mRNAs of the ubiquitin-proteasome proteolytic pathway in human skeletal muscle*. J Clin Invest. 1997; **99**: 163–168.
- ³⁵ Bossola M., Muscaritoli M., Costelli P., Bellantone R., Pacelli F., Busquets S., Argilès J., Lopez-Soriano F.J., Civello I.M., Baccino F.M., Fanelli F.R., and Doglietto G.B. *Increased muscle ubiquitin mRNA levels in gastric cancer patients*. Am. J. Physiol. Regul. Integr. Comp. Physiol. 2001; **280**: R1518-R1523.
- ³⁶ Yimlamai T., Dodd S.L., Borst S.E., Park S. *Clenbuterol induces muscle-specific attenuation of atrophy through effects on the ubiquitin-proteasome pathway*. J Appl Physiol. 2005; **99**:71-80.
- ³⁷ Kwakl K.S., Zhou X., Solomon V., Baracos V.E., Davis J., Bannon A.W., Boyle W.J. , Lacey D.L., and Han H.Q. *Regulation of Protein Catabolism by Muscle-Specific and Cytokine-Inducible Ubiquitin Ligase E3a-II during Cancer Cachexia*. Cancer Res. 2004; **64**; 8193-97.
- ³⁸ Fischer D., Sun X., Gang G., Pritts T. and Hasselgren P. *The Gene Expression of Ubiquitin Ligase E3a Is Upregulated in Skeletal Muscle during Sepsis in Rats—Potential Role of Glucocorticoids*. Biochemical and Biophysical Research Communications. 2000; **267**:2, 504-508.
- ³⁹ Adegoke O.A., Bedard N., Roest H.P., and S.S.Wing. *E214k, the N-end rule ubiquitin conjugating enzyme, is dispensable for the increase in protein catabolism in muscle of fasted mice*. Am J Physiol Endocrinol Metab, 2002; **10**: 97.
- ⁴⁰ Kwon Y.T., Xia Z., Davydov I.V., Lecker S.H., and Varshavsky A. *Construction and analysis of mouse strains lacking the ubiquitin ligase UBR1 (E3) of the N-end rule pathway*. Mol. Cell Biol. 2001; **21**: 8007–8021.
- ⁴¹ Singhal S., Taylor M.C., Baker R.T. *Deubiquitylating enzymes and disease*. BMC Biochem. 2008; **21**;9-15.
- ⁴² Dayal S., Sparks A., Jacob J., Allende-Vega N., Lane D.P., Saville M.K. *Suppression of the deubiquitinating enzyme USP5 causes the accumulation of unanchored polyubiquitin and the activation of p53*. J Biol Chem. 2009; **284**(8):5030-41.
- ⁴³ Wang T., Yin L., Cooper E.M., Lai M.Y., Dickey S., Pickart C.M., Fushman D., Wilkinson K.D., Cohen R.E., Wolberger C. *Evidence for bidentate substrate binding as the basis for the K48 linkage specificity of otubain I*. J Mol Biol. 2009; **386**(4):1011-23.

-
- ⁴⁴ Sato Y., Yoshikawa A., Yamagata A., Mimura H., Yamashita M., Ookata K., Nureki O., Iwai K., Komada M., Fukai S. *Structural basis for specific cleavage of Lys 63-linked polyubiquitin chains*. Nature. 2008; **455**, 358-362.
- ⁴⁵ Rivett, A.J., Hearn, A.R. *Proteasome function in antigen presentation: immunoproteasome complexes, Peptide production, and interactions with viral proteins*. Curr. Protein Pept. Sci. 2004; **5**: 153–161.
- ⁴⁶ Zhong X. and R.N. Pittman. *Ataxin-3 binds VCP/p97 and regulates retrotranslocation of ERAD substrates*. Human Molecular Genetics. 2006; **15(16)**:2409-2420.
- ⁴⁷ Hassink G.C., Zhao B., Sompallae R., Altun M., Gastaldello S., Zinin N.V., Masucci M.G., Lindsten K. *The ER-resident ubiquitin-specific protease 19 participates in the UPR and rescues ERAD substrates*. EMBO Rep. 2009; **10(7)**:755-61.
- ⁴⁸ Peng, J. S. D., Elias, J. E., Thoreen, C. C., Cheng, D., Marsischky, G., Roelofs, J., Finley, D., and Gygi, S. P. *A proteomics approach to understanding protein ubiquitination*. Nat. Biotechnol. 2003; **21**: 921–926.
- ⁴⁹ Winborn B.J., Travis S.M., Todi S.V., Scaglione K.M., Xu P., Williams A.J., Cohen R.E., Peng J., Paulson H.L. *The deubiquitinating enzyme ataxin-3, a polyglutamine disease protein, edits Lys63 linkages in mixed linkage ubiquitin chains*. J. Biol Chem. 2008; **283(39)**:26436-43.
- ⁵⁰ Lam, Y. A., Xu, W., DeMartino, G. N., and Cohen, R. E. *Editing of ubiquitin conjugates by an isopeptidase in the 26S proteasome*. Nature. 1997; **385**: 737–740.
- ⁵¹ Verma R., Aravind L., Oania R., McDonald W.H., Yates J.R. 3rd, Koonin E.V., Deshaies R.J. *Role of Rpn11 Metalloprotease in Deubiquitination and Degradation by the 26S Proteasome*. Science. 2002; **298**: 611 – 615.
- ⁵² Combaret L., Adegoke O.A., Bedard N., Baracos V., Attaix D., Wing SS. *USP19 is a ubiquitin-specific protease regulated in rat skeletal muscle during catabolic states*. Am J Physiol Endocrinol Metab. 2005; **288(4)**:E693-700.
- ⁵³ Sundaram P., Pang Z., Miao M., Yu L., Wing S.S. *USP19-deubiquitinating enzyme regulates levels of major myofibrillar proteins in L6 muscle cells*. Am J Physiol Endocrinol Metab. 2009; **297(6)**:E1283-90.
- ⁵⁴ Adhietty P.J., O'Leary M.F.N., Chabi B., Wicks K.L. and D.A. Hood. *Effect of denervation on mitochondrially mediated apoptosis in skeletal muscle*. J Appl Physiol. 2006; **102**:1143-1151.
- ⁵⁵ Borisov A.B. and Carlson B.M. *Cell Death in Denervated Skeletal Muscle Is Distinct From Classical Apoptosis*. The Anatomical Record. 2000; **258**:305–318
- ⁵⁶ Tews, D.S. *Apoptosis and muscle fiber loss in neuromuscular disorders*. Neuromuscular Disorders. 2002; **12**: 613–622.